Annual Report | *January 1, 1966 – December 31, 1966*

RESPONSE OF A BURNING PROPELLANT SURFACE TO EROSIVE TRANSIENTS

Prepared for:

AIR FORCE OFFICE OF SCIENTIFIC RESEARCH
WASHINGTON, D.C. 20333

CONTRACT NO. AF 49(638)-1665

STANFORD RESEARCH INSTITUTE

MENLO PARK, CALIFORNIA

*SRI

Form 1473

(9) Annual Report, 1 Jan [redacted] – Dec [redacted] 66, (31)

(6) RESPONSE OF A BURNING PROPELLANT SURFACE TO EROSIVE TRANSIENTS.

Prepared for:

AIR FORCE OFFICE OF SCIENTIFIC RESEARCH
WASHINGTON, D.C. 20333

(15) CONTR[redacted]. AF 49(638)-1665

(10) [redacted] E. L. CAPENER (twin), L. A. DICKINSON (ionel), R. J. KIER (oger), G. A. MARXMAN (erald), C. E. WOOLDRIDGE (harles)

(16) SRI-[redacted]FRU-5818

(11) 31 Dec 66

(12) 62p.

Approved: LIONEL A. DICKINSON, DIRECTOR
POLYMER & PROPULSION SCIENCES DIVISION

Copy No. 74

mt

(332 500) JE

FOREWORD

The experimental and theoretical studies described in this report are the responsibilities of K. L. Capener and G. A. Marxman, respectively. The overall program is under the direction of L. A. Dickinson.

The program is under the overall management of the Air Force Office of Scientific Research, Directorate of Engineering Sciences, Propulsion Division, (B. T. Wolfson).

The major contributions of C. E. Wooldridge and R. J. Kier to the program are gratefully acknowledged. The supplementary information on propellant ignition characteristics was derived from studies performed by N. Fishman.

SYNOPSIS

The study of the combustion instability of solid propellants has as its ultimate goal the development of a method for predicting whether a new propellant will be susceptible to combustion instability. In the studies done under this present contract, significant progress has been made in correlating finite amplitude axial mode instability with a theoretical analysis of the combustion wave. When laboratory derived physical-chemical propellant data are substituted in the appropriate expressions, it has proved possible to predict in a qualitative manner the unstable response of a propellant.

The studies this year have been concerned with improving the combustion model, interpreting the fluid dynamic phenomena, and experimentally determining the magnitude of critical ballistic parameters. In order to verify that solid-phase reactions were occurring, differential thermal analysis studies were performed on selected propellants at pressures up to 70 atmospheres. A quadrapole mass spectrometer was used to distinguish between condensed-phase and gas-phase reactions. With ammonium perchlorate propellants, a solid-phase heat release of up to 200 calories per gram was observed.

An examination of the wave structure obtained in both tubular and opposed slab rocket motors indicates that the finite amplitude wave is a shock wave (supported by mass and energy addition in the wake).

In the continuing development of the analytical model of the combustion wave, the justification of the physical assumptions made in developing a mathematically tractable theory have been critically reviewed and compared with those of other workers.

TABLE OF CONTENTS

LIST OF ILLUSTRATIONS

LIST OF TABLES

LIST OF SYMBOLS*

a frequency factor in Arrhenius law Eq. (2)

A solid-phase kinetics parameter defined by Eq. (12)

B parameter defined by Eq. (12)

c coefficient in empirical burning rate law, $r = cp^{\nu}$

C constant defined by Eq. (7)

c_p specific heat capacity of gas at constant pressure

c_s specific heat capacity of solid

E activation energy for pyrolysis at the interface Eq. (2)

E_D activation energy for pressure-insensitive surface-coupled reactions, Eq. (9)

E_f activation energy for gas-phase reaction, Eq. (7)

E_H activation energy for pressure-sensitive surface-coupled reactions, Eq. (8)

h enthalpy

h_{g_w} = energy carried into gas phase with the vaporizing propellant per unit mass

h_{s_w} = energy carried by convection from the unreacted solid phase per unit mass

H_D heat release (positive)/unit mass propellant in pressure-insensitive surface coupled reactions, Eq. (9)

H_H heat release (positive)/unit mass propellant (at a reference temperature and pressure) in pressure-sensitive surface-coupled reactions, Eq. (8)

*Equation numbers refer to the Appendix.

LIST OF SYMBOLS (Cont'd)

K	thermal diffusivity of solid = $k/\rho_s c_s$
k	thermal conductivity of solid
L	heat of vaporization/unit mass of propellant
m	order of heterogeneous reaction Eq. (8); mass flux from the wall
M	Mach number
n	order of gas-phase reaction, Eq. (7)
p	chamber pressure
q	parameter defined by Eq. (17)
Q_D	heat of reaction/unit mass of reactant in the pressure-insensitive surface-coupled reaction
Q_H	heat of reaction/unit mass of reactant in the pressure-sensitive surface-coupled reaction
Q_r	heat of reaction/unit mass of reactant in the gas-phase reaction
Q_T	total heat of combustion
R	gas constant
r	burning rate
T	temperature
t	time
x	distance into the propellant from its surface

Greek letters

α	gas-phase kinetics parameter defined by Eq. (12)
γ	specific heat ratio c_p/c_v
ϵ	amplitude of pressure oscillation, Eq. (15)
ϵ_r	mass fraction of reactant at the propellant surface (nearly unity)
θ_D	parameter defined by Eq. (15)
θ_H	parameter defined by Eq. (14)
ϑ_s	parameter defined by Eq. (13)
ν	pressure exponent in empirical burning rate law, $r = cp^{\nu}$
ρ_s	density of solid propellant

ϕ phase angle between perturbed mass flux and perturbed pressure

χ number of sites which undergo surface-coupled reactions per unit mass of solid propellant

Subscripts

f gas-phase flame

g gas phase

o conditions at $x \to \infty$

s solid phase

w conditions at the wall (gas-solid interface)

Superscripts

(-) denotes value of quantity prior to pressure disturbance

($\sim$) denotes difference between perturbed and unperturbed value, divided by unperturbed value; $\tilde{r} = (r(t) - \bar{r})/\bar{r}$.

I INTRODUCTION AND SUMMARY

The long-range goal of these theoretical and experimental studies on the combustion instability characteristics of solid propellants is the development of a method for predicting, at an early stage in a research program, whether a new propellant will be susceptible to certain types of combustion instability. In the studies performed under the present contract, significant progress has been made in correlating finite-amplitude axial-mode instability with a theoretical analysis of the combustion wave. Furthermore, when laboratory-derived physical-chemical propellant data are substituted into the appropriate expressions, it is possible to compute the critical frequency-response spectrum for a propellant. In addition, when the energy-release distribution within the condensed and gaseous phases is examined, the relative magnitude of the unstable response can be predicted.

This year our studies have been concerned with improving the combustion model, interpreting the fluid dynamic phenomena, and experimentally determining the magnitude of critical ballistic parameters. In a previous report[1] it was shown that solid-phase reactions may be a controlling factor in the incidence of instability. This hypothesis was advanced on the basis of a relatively comprehensive theoretical analysis, and it was considered necessary to unequivocally verify its significance by experimental studies. Accordingly, differential thermal analysis studies were performed on selected propellants at pressures up to 70 atmospheres; the DTA cell was monitored with a quadrapole mass spectrometer in order to distinguish between condensed-phase and gas-phase reactions. The results showed that ammonium perchlorate based propellants react partially in the condensed state, releasing up to 200 calories per gram. Supporting evidence for exothermic condensed-phase reactions was also obtained from thermocouple studies.

A thorough examination of the wave structure obtained in both tubular and opposed slab rocket motors suggests very strongly that the finite-

amplitude wave is a shock wave (supported by mass and energy addition in the wake) rather than a Chapman-Jouget detonation in the gas phase.

In the continuing development of the analytical model of the combustion wave, the physical assumptions used in developing a mathematically tractable theory have been critically reviewed and compared with those of other workers. This review indicates that the present combustion model (which allows for condensed-phase or surface-coupled heat release) differs from earlier treatments primarily in the assumptions concerning the surface kinetics. Owing to this difference, the present theory appears to be the only one capable of distinguishing between composite and double base propellants, which our experimental studies have shown to have very different stability characteristics. On the basis of currently available information, the present model represents a reasonably realistic, though still highly simplified, representation of the combustion process; furthermore, it is amenable to a clear interpretation in terms of basic physical and chemical mechanisms.

II EXPERIMENTAL STUDIES

The experimental studies performed have been concerned with both the microballistic phenomena of the combustion processes and the macroballistic behavior of large rocket motors.

Our study of microballistic phenomena has been directed toward elucidating the nature of condensed-phase reactions and determining whether any important gas-phase processes can be studied by rapid scan spectroscopy.

A series of opposed slab motors were test fired to gain data on fluid dynamic propagation characteristics of finite amplitude waves generated with a variety of propellants.

An examination of the physical phenomena observed experimentally in our test motors has been made from the standpoint of established gas dynamic theory.

A. Condensed Phase Exothermic Reactions in Solid Propellants

In order to explain the occurrence of finite-amplitude axial-wave instability observed with composite propellants, a combustion model which characterizes the transient response of a propellant was developed.[2] It was observed that instability in composite propellants was invariably associated with the presence of ammonium perchlorate (additional requirements in relation to burning rate and pressure were also noted[1,2]). In interpretating the experimental studies performed, it was postulated that heat release associated with certain solid-phase reactions involving ammonium perchlorate were responsible for axial mode instability in the frequency range studied (200-2000 cps); the theoretical treatment developed used this concept of solid-phase reactions to modify Denison and Baum's analysis[3] and successfully qualitatively predicted the observed behavior.

It was considered desirable to unequivocally demonstrate that solid-phase reactions in ammonium perchlorate propellants released energy at

the level required by the theory and that the concept of solid-phase heat release from oxidizer decomposition and associated heterogeneous redox reactions was not an imaginary physical concept generated to explain the experimental behavior or satisfy the demands of an elegant mathematical analysis. It will be recalled that on the basis of temperature profile measurements obtained using fine wire thermocouples, Summerfield[4] inferred a solid-phase heat release of about 230 cal/gram for one propellant containing 70% AP..

In this present work differential thermal analysis (DTA) studies combined with mass spectrographic analysis of gaseous decomposition products were used to differentiate between gas-phase reactions and solid-phase reactions which might occur during the decomposition of ammonium perchlorate and potassium perchlorate based propellants. These studies were performed at a series of pressures ranging from one to seventy atmospheres. Arc image furnace (AIF) heating studies were performed to further confirm the existence of significant reactions within the solid phase in ammonium perchlorate propellants and their absence in potassium perchlorate propellants.

1. DTA-Mass Spectrographic Studies

A DTA cell designed to operate at elevated pressures was fabricated; its detailed construction is shown in Fig. 1. The cell is fitted with safety rupture diaphragms. The decomposition off-gases can, when desired, be ducted to an analytical mass spectrometer. In the studies performed, a quadrupole residual gas analyzer (Electrical Associates Incorporated, Quad 210) was used.

DTA thermograms were first obtained for both production grade ammonium perchlorate and purified ammonium perchlorate. The main difference in composition is that the chlorate ion concentration is significantly lower in the purified materials. Figure 2 shows the thermograms characteristic of production grade ammonium perchlorate (heated at a rate of 10°C/min) at pressures of one atmosphere (14.7 psia) and 34 atmospheres (500 psia). At one atmosphere a pre-deflagration exotherm is found at 300°C, followed by the deflagration exotherm at

approximately 400°C; the crystal transformation endotherm appears at 240°C. At 34 atmospheres the deflagration exotherm is coincident with the low pressure pre-deflagration exotherm. When highly purified ammonium perchlorate is examined (Fig. 3), the only exotherm observed at either pressure is that associated with deflagration; at one atmosphere this occurs at 425°C, and at 34 atmospheres this exotherm shifts to a lower temperature of 325°C (some 25°C above the corresponding point on the thermogram of the production grade AP).

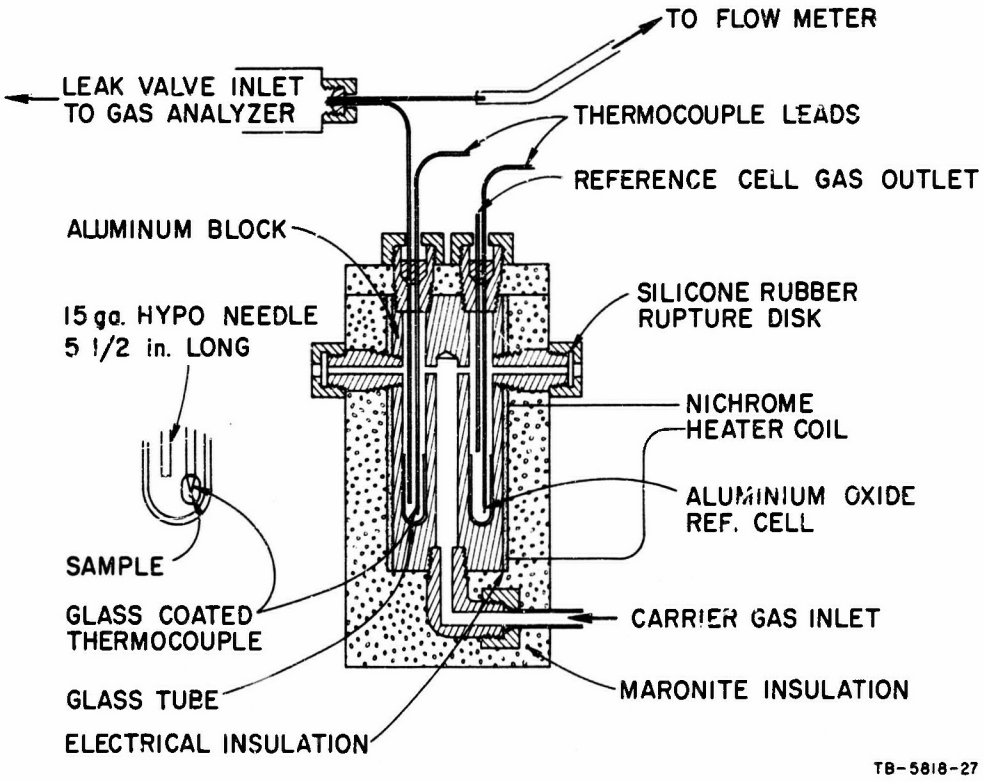

FIG. 1 HIGH PRESSURE DTA CELL

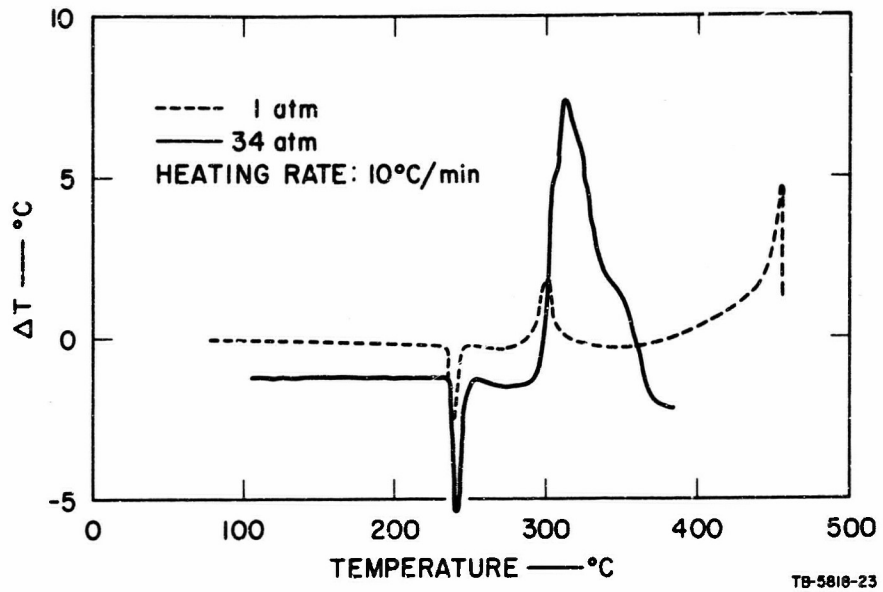

FIG. 2 THERMOGRAMS FOR PRODUCTION GRADE AMMONIUM PERCHLORATE

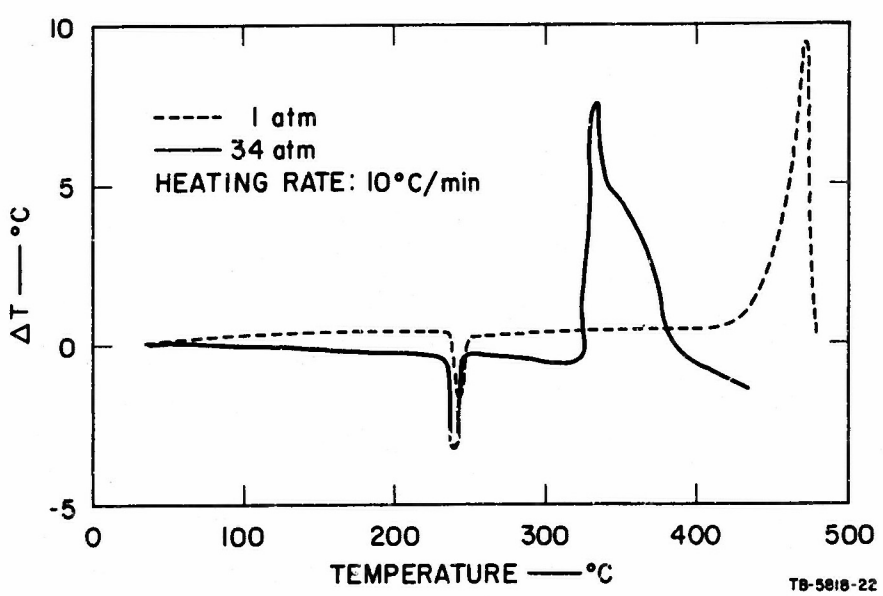

FIG. 3 THERMOGRAMS FOR HIGH PURITY AMMONIUM PERCHLORATE

With the background data established for ammonium perchlorate, the influence of pressure on DTA thermograms was carefully studied for a specially prepared propellant. This contained 70% by weight of the highly purified ammonium perchlorate and 30% by weight of a specially purified hydroxy terminated polybutadiene based binder prepared from a polybutadiene polymer (Poly-B.D. R-45, Sinclair Petrochemicals) and toluene di-isocyanate. (The choice of highly purified ingredients is critical for the clean separation of the observed exotherms.)

This special propellant was studied in the DTA cell at pressures up to 70 atmospheres (1000 psia), and the data are shown in Fig. 4. At pressures up to 25 atmospheres (350 psia) two or more exotherm peaks occur; the first, at 350-360°C, is unaffected by pressure change, but as the pressure is increased above 25 atmospheres, the exotherms appear at successively lower temperatures until at 34 atmospheres (500 psia) only one deflagration exotherm is recorded.

In order to gain additional information to help explain observed phenomena, the DTA sample capillary was swept with a carrier gas (nitrogen) which was sampled continuously through the quadrupole residual gas analyser. This instrument uses a quadrupole and rf electric field for mass analysis, and provides a rapid response of about 10 milliseconds when scanning the mass range 0-50. All tests were done at atmospheric pressure in order to obtain maximum separation of the exotherms. Any gaseous decomposition products were continuously monitored as the sample temperature increased. The gas transit time through the hot sampling capillary was approximately one second, whereas the duration of a typical exotherm was of the order of four minutes; thus for all practical purposes sample analysis was instantaneous. Gas sampling data for the production grade AP (this did not contain an anticaking agent) are given in Table I. Little gas evolution occurred until the deflagration exotherm commenced above 400°C. A very slight amount of oxygen (less than 10^{-6} moles/100 grams sample) came off during the pre-decomposition exotherm. We conclude therefore that this is primarily a solid-phase exotherm resulting from decomposition or reaction of trace contaminants; sodium chlorate is a

likely candidate,

$$NaClO_3 \longrightarrow NaClO_4 + \tfrac{1}{2}O_2$$

Other unidentified organic contaminants introduced during preparation of ammonium perchlorate may also contribute to this pre-deflagration exotherm.

TABLE I

MASS SPECTROGRAPHIC
GAS ANALYSIS OF PRODUCTION GRADE

Species Detected		Mass to Charge Ratio m/e
at 310°C	at 460°C	
	H_2O^+	18
	N_2^+	28
	NO^+	30
Trace O_2	O_2^+	32
	HCl^+	36
	N_2O^+	44

The experimental results were about the same for the special propellant studied. The thermograms are shown in Fig. 5, and the gas analysis data are given in Table II. The data for the first exotherm at between 360°C and 368°C established that hardly any gas other than trace amounts of water and carbon dioxide evolved. Thus the first exotherm is apparently a condensed-phase reaction little affected by pressure. Significant gas evolution is associated with the other exotherms.

Relating the data on the first exotherm to the observed trends in behavior shown for the propellant in Fig. 4, it is surmised that, over the interval of 15 to 350 psia, pressure sensitivity causes the trailing exotherms to move to lower temperatures until at 500 psia the gas-phase reactions predominate.

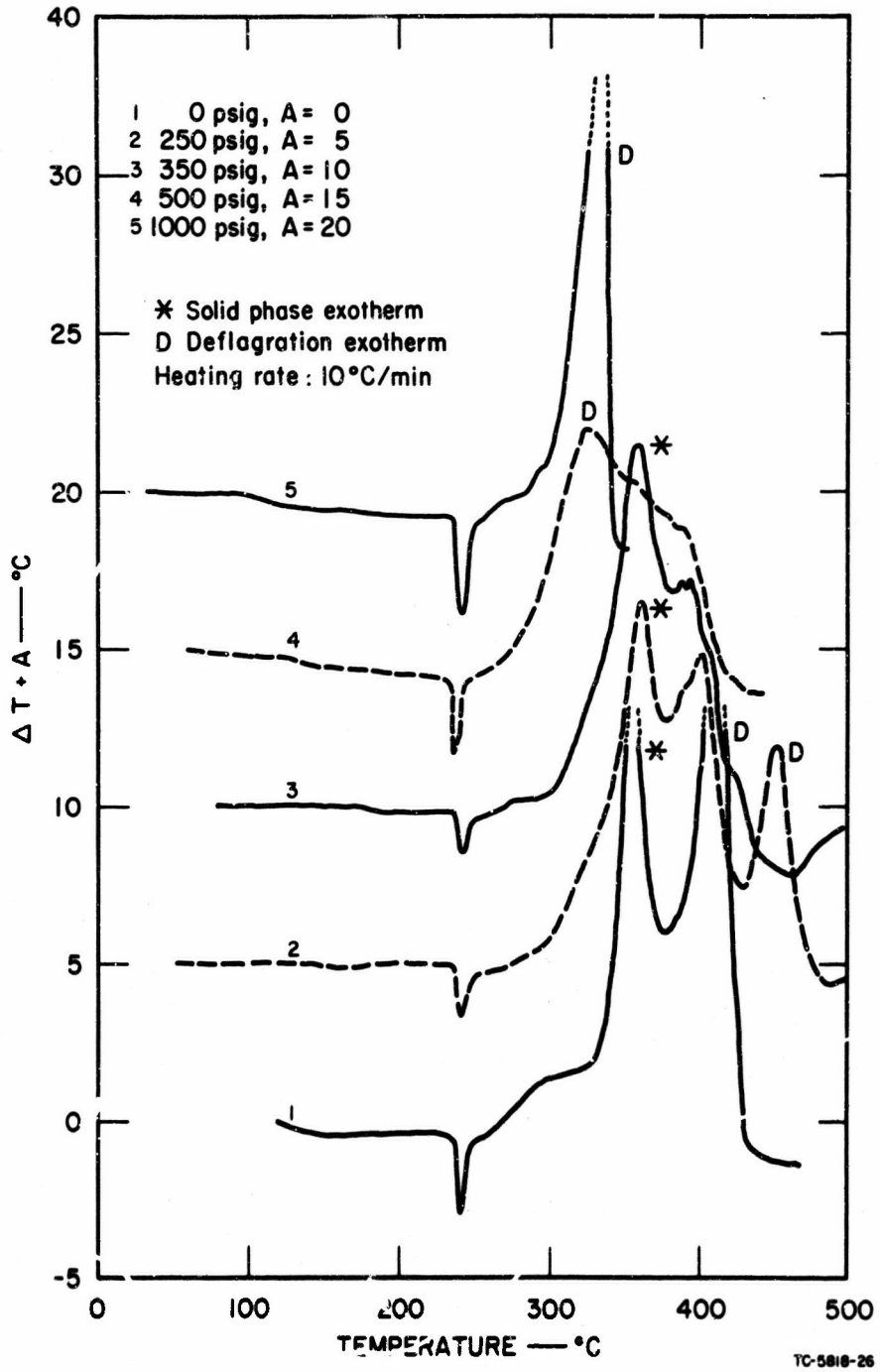

FIG. 4 THERMOGRAMS FOR PURIFIED PROPELLANTS AT AMBIENT AND ELEVATED PRESSURES

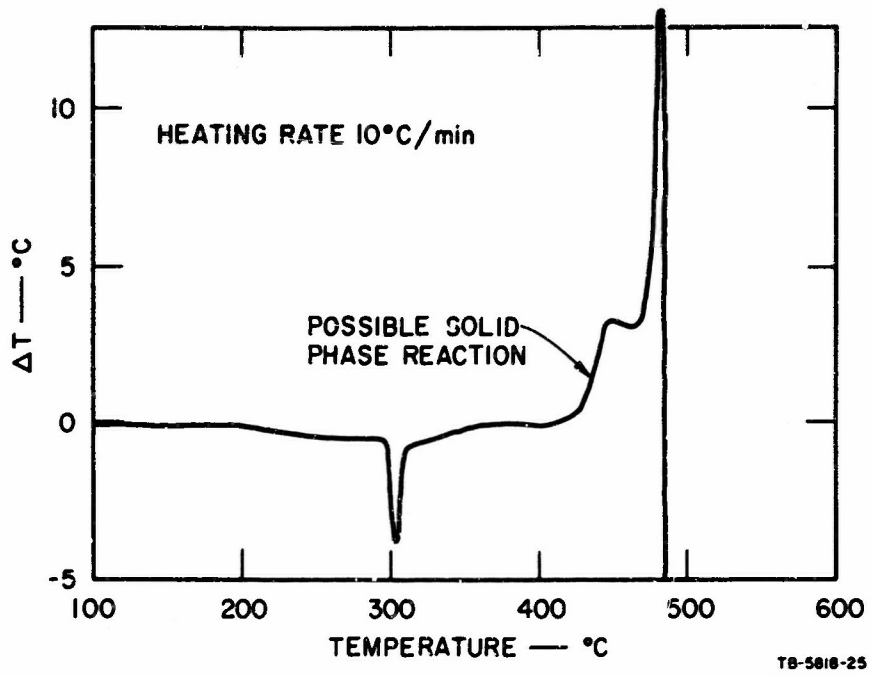

FIG. 5 THERMOGRAM FOR POTASSIUM PERCHLORATE BASED PROPELLANT

By using the known endotherm of 2.3 kcal/mole for the ammonium perchlorate crystal change,[5] (identified as the DTA endotherm at 240°C) it is feasible to estimate the percentage of total heat release contributed by the solid-phase exotherm. Since neither the endotherm nor exotherm is associated with the generation of any gases (which would result in mass changes and heat transport), it is considered permissible to relate the areas beneath the endotherm and exotherm of the DTA thermogram to the amounts of heat released or absorbed.[6] Thus the thermogram at atmospheric pressure indicates that the condensed-phase reaction heat release for the propellant studied is 0.172 kcal/g. This is approximately 18% of the total heat release during explosion, 0.94 kcal/g, as measured in a calorimeter.

TABLE II

MASS SPECTROGRAPHIC
GAS ANALYSIS OF 70/30 HIGH PURITY AP/POLYBUTADIENE PROPELLANT

Species Detected		Mass to Charge Ratio m/e
at 360°C	at 410°C	
	H_2^+	2
	C^+	12
	NH^+, CH_3^+	15
Trace H_2O^+	H_2O^+	18
	C_2	24
	CN^+	26
	HCN^+	27
	NO^+, CH_2O^+	30
	O_2^+	32
	HCL^+, C_3^+	36
Trace CO_2^+	CO_2^+	44

Is is of significance that DTA thermograms for potassium perchlorate and potassium perchlorate propellants showed only a deflagration exotherm (a typical thermogram is shown in Fig. 5). Even a liberal estimate of the heat release associated with solid-phase reactions in the propellant would not be above 5% of the total heat of explosion.

It is noteworthy that a composite propellant based on ammonium perchlorate and a fluorocarbon binder exhibits the same ambient pressure DTA-thermogram as a conventional propellant (Fig. 6). By analogy, therefore, it is predicted that the fluorocarbon/AP propellant and the conventional composite propellant will be unstable over much the same pressure/burning rate spectrum.

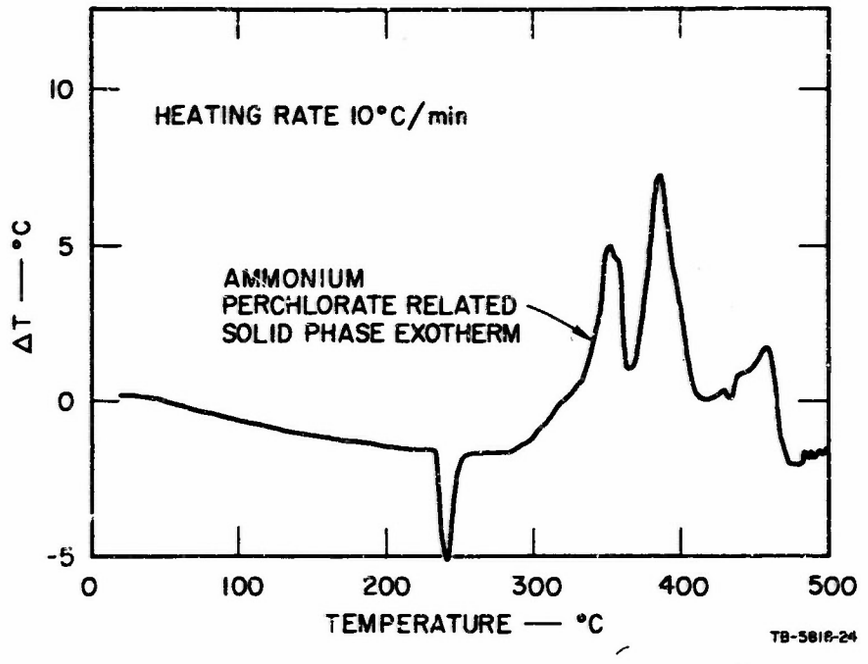

FIG. 6 THERMOGRAM FOR FLUOROCARBON BASED PROPELLANT

2. Arc Image Furnace Studies

A particularly useful means of characterizing the ignition behavior of a solid propellant is to plot the logarithm of the exposure time to radiant flux versus the logarithm of the flux. When experimental data fall on a line of slope equal to -2 on such a plot, and if there is no chemical reaction, ignition can be characterized by a constant surface temperature which is independent of flux. In AIF studies of several operational and model propellant compositions,[8] we observed that test data were generally well fit by such a line of -2 slope up to a certain critical value of flux; at higher fluxes the data deviated toward larger values of time. Subsequent work[7,8] (supported by Stanford Research Institute) with embedded surface thermocouples showed that surface exotherms could be detected in ammonium perchlorate propellants prior to ignition at incident fluxes above the critical flux. Further, no exotherm could be detected under test conditions where the log time vs log flux data were fit by a line of -2 slope.

The compositions of the propellants for this AIF study are given in Table III. The ignition time versus energy flux plots for the potassium perchlorate and ammonium perchlorate based propellants are shown in Figs. 7 and 8. It is found that both propellants show a point of inflexion at a certain critical flux. Beyond the point of inflexion time to ignition includes the exposure time plus an induction time. The thermocouple data to be described were obtained for each propellant under comparable conditions; the data obtained at the points marked by X on Figs. 7 and 8 are typical for ignition behavior at fluxes beyond the inflexion point.

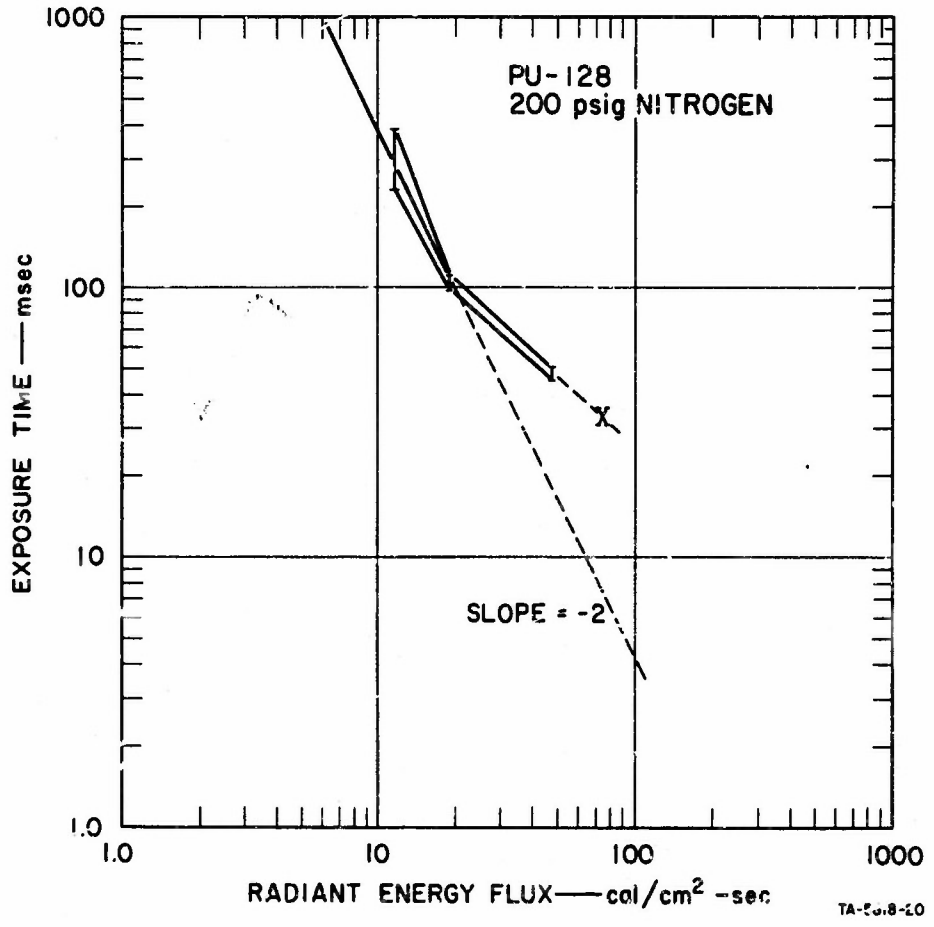

FIG. 7 ARC IMAGE FURNACE IGNITION CHARACTERISTICS OF A $KClO_4$ PROPELLANT: PU-128

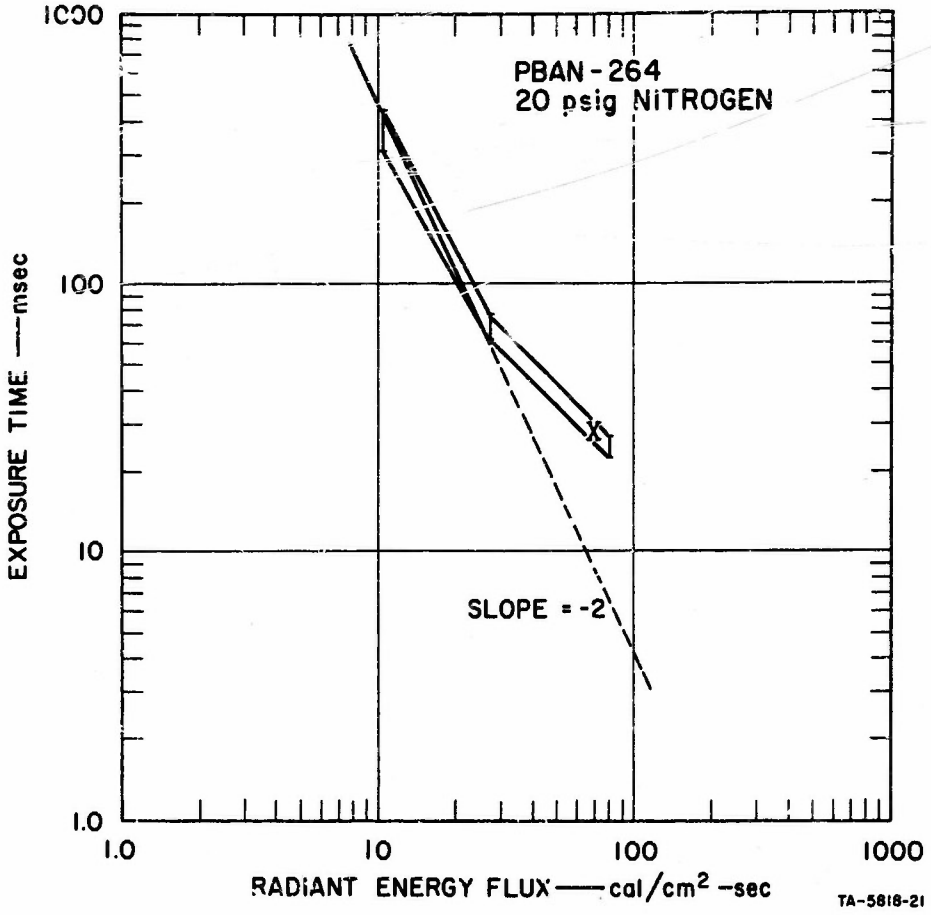

FIG. 8 ARC IMAGE FURNACE IGNITION CHARACTERISTICS OF AN NH_4ClO_4 PROPELLANT: PBAN-264

The surface layer thermocouple data for the potassium perchlorate based propellant are shown in Fig. 9; those for the ammonium perchlorate based propellant are shown in Fig. 10. In examining Fig. 9 we see that after the initiation of the energy pulse at time i the temperature rises progressively until the pulse terminates at time t. At this time the surface layer loses heat principally by conduction into the body of the sample, but ultimately a runaway deflagration occurs at time r. The temperature-time trace shows that heating of the sample occurs only by the external stimulus of the incident radiant energy.

TABLE III

PROPELLANT COMPOSITIONS FOR AIF STUDIES

Ingredient	PBAN 264	PU 128
AP (150 μ)	59.5	-
AP (11 μ)	25.5	-
KP (150 μ)	-	56.0
KP (11 μ)	-	22.0
PBAN Binder	15.0	-
Polyurethane Binder	-	22.0

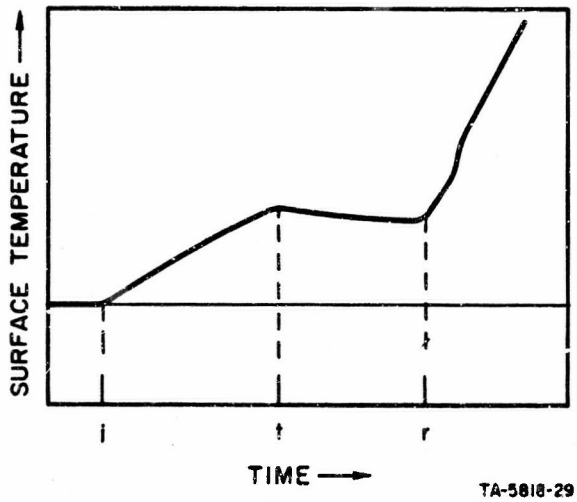

FIG. 9 EMBEDDED SURFACE THERMOCOUPLE RESPONSE DURING IGNITION OF PU-128

A completely different response occurs in the case of the AP propellant as is shown in Fig. 10. Following initiation of the energy pulse (time i), the temperature rises steadily, and at time e an inflexion occurs which can only be interpreted as the onset of condensed phase exothermic reactions. On termination of the energy pulse, time t, the temperature continues to rise because of the exothermic reaction, and a runaway deflagration (ignition) occurs at time r.

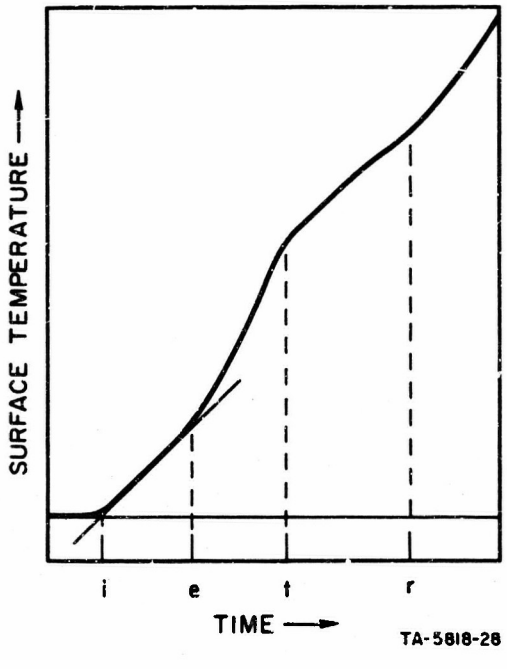

FIG. 10 EMBEDDED SURFACE THERMOCOUPLE RESPONSE DURING IGNITION OF PBAN-264

The differences in behavior of the potassium and ammonium perchlorate based propellants during an ignition event are considered to clearly indicate that significant condensed-phase reactions only occur in the AP based propellants. A thermal analysis of thermocouple data using the method of Sabadell et al.[4] suggests that the condensed-phase heat release is of the order of 200 cal/g.

3. Conclusions

Both the differential thermal analysis studies and thermocouple studies of the ignition process indicate that up to 18% of the total heat of explosion occurs within the solid phase during the combustion of ammonium perchlorate based composite propellants. These data justify the hypothesis previously advanced[1] that combustion instability in composite propellants is related to the level of solid-phase heat release and supports the theoretical transient response analysis[2] which incorporates condensed-phase heat release and related solid-phase kinetics as necessary components of the combustion wave model.

B. Spectroscopic Studies of Solid Propellant Combustion Phenomena Inside Rocket Motors

In order to study the interaction of finite amplitude waves generated during combustion instability with gas-phase processes at the burning surface, consideration was given to examining them with a rapid scan spectroscope. Other investigators have found it very difficult to record spectra of combustion of solid propellants at elevated pressures. For example, above a pressure of about 50 psia, most workers have found the emission spectra to be obscured by a carbon continuum.[9,10] An examination of numerous spectra has disclosed that sodium and calcium emission lines are also extremely prominent, and their presence, even under steady state conditions, prevents the use of exposure times long enough to record lines of lesser intensity on photographic recording plates. Another problem which interferes with our understanding of the spectra is that increasing the combustion pressure causes lines to broaden into bands. In many cases the bands overlap, and there is therefore an immense difficulty in interpretation. To surmount the above difficulties, along

with the problem of tracking a traveling wave within a motor and obtaining a spectral record within microseconds rather than seconds, appeared to be a formidable problem. However, the recent introduction of the technique of recording spectra by use of image converter or image dissector tubes has provided a means of recording spectra in microseconds (60 μ or less). Thus the remaining problems were examined more closely for solutions.

A probing experiment was first conducted to record the spectra from the combustion zone in a solid propellant rocket motor. This motor was of the slab configuration reported previously and contained an 80/20 ammonium perchlorate/PBAN binder. The experimental set-up is shown in Fig. 11. Flame spectra taken when the combustion pressure was 1400 psig were of extremely poor contrast and not suitable for reproduction. However, it was possible to identify nearly all the bands or lines which are almost obscured by the carbon continuum as contaminants in the propellant ingredients. Sodium and calcium appear to be responsible for most of the spectral activity observed. Sodium is a contaminant in ammonium perchlorate and the calcium is derived from tricalcium phosphate used as an anticaking agent. Both are removable to a degree. Whether this influences the spectra significantly was the subject of further screening experiments using a vidicon tube to record the spectra from a prism or grating and using highly purified AP based propellants; both a prism and grating were used with the vidicon tube. A high pressure burner was also used as the primary test apparatus in order to minimize the experimental costs.

Initial experiments have been concerned with evaluating optical systems and vidicon tube sensitivities, as well as examines propellant spectra. In Fig. 12 we compare the spectra, taken in 60 microseconds, of a propellant made from high purity ammonium perchlorate and of a propellant made from production grade material containing tricalcium phosphate; both samples were burned at a pressure of 500 psig. This experiment indicates that elimination of easily ionizable elements from AP by repeated crystallization may make spectral identification of key reactions easier if the sensitivity of the vidicon tube can be increased significantly. A literature search has disclosed that this is possible by using an image dissector tube rather than the vidicon tube.

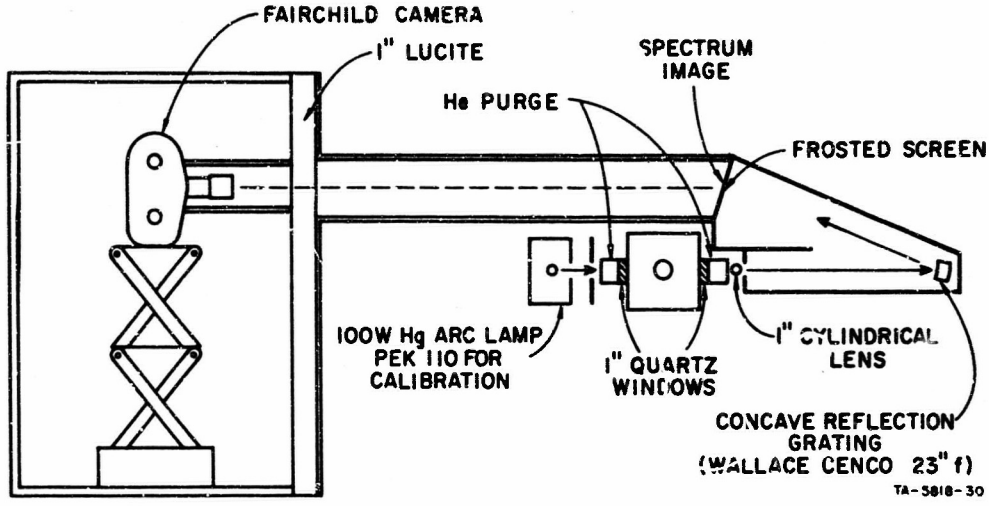

FIG. 11 APPARATUS FOR EMISSION SPECTROSCOPY

C. Wave Growth Studies

1. Influence of Aluminum on Gas Dampening

Several experiments were conducted in 5-in. x 80-in. slab motors to measure the w e pressure and velocity at different stations. The propellant variable was aluminum content, 5% versus 15%. Data on the 15% Al loaded propellant were lost because of Kistler gage instabilities induced by high temperature; neither the wave pressure nor velocity profile could be deduced. At the four out of six stations which functioned adequately, it was apparent that the wave pressure was significantly reduced; this test has to be repeated. Unfortunately, under the severe conditions of heat transfer, neither motor tube nor pressure gages last very long.

The test with propellant containing 5% aluminum was more successful in that the wave pressure was tracked successfully. However, one gage was lost, and so again the velocity profile could not be deduced.

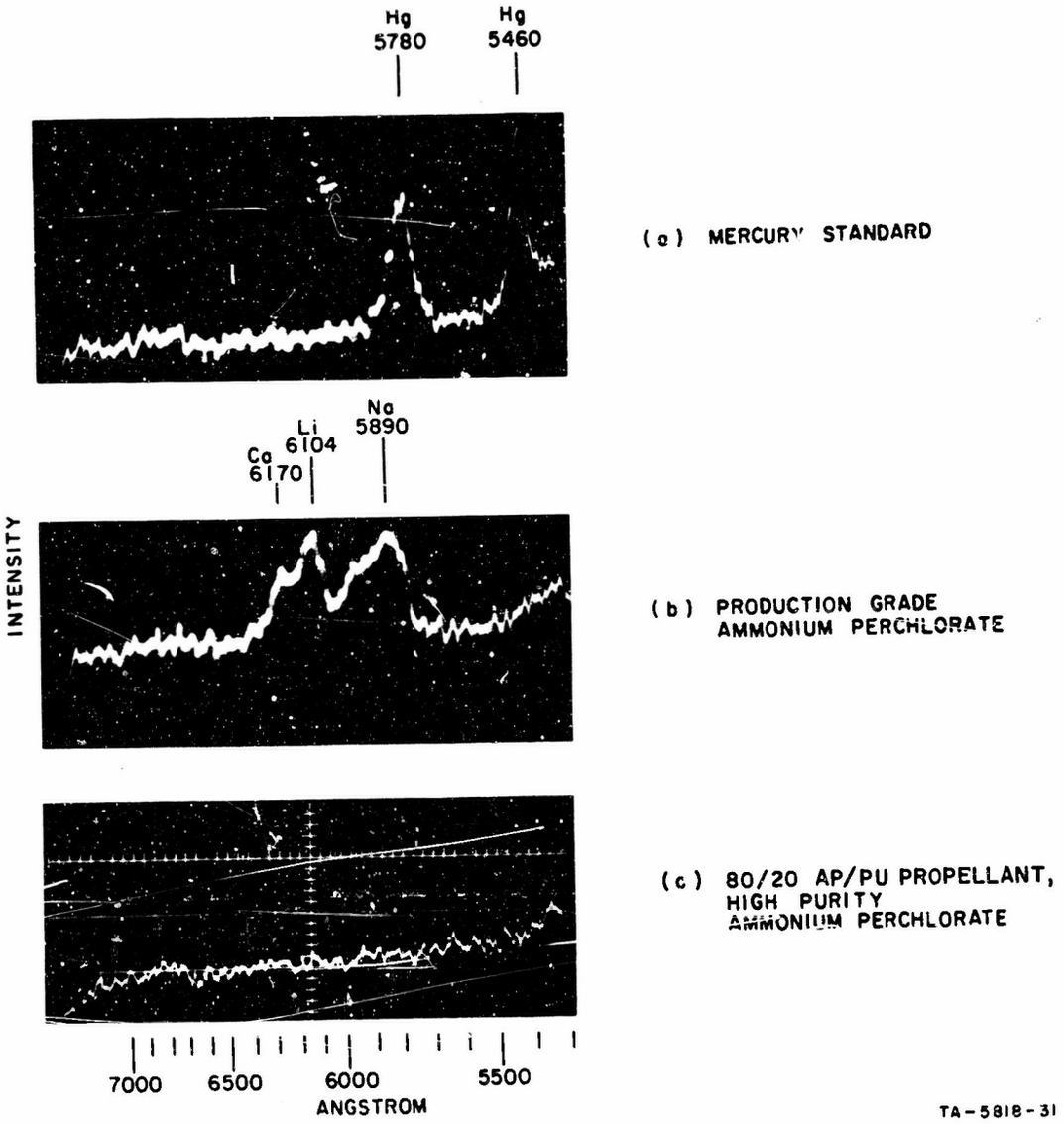

FIG. 12 HIGH SPEED SPECTROSCOPY RESULTS

This propellant generated higher wave pressures and exhibited higher gain factors than did the 80/20 AP/binder propellant reported in a previous Annual Report.[8]

In our study[2] of wave pressure and velocity in the 5-in.-diameter motors the combustion in the 15-in. motor did not go unstable, and we were unable to track the pulse beyond one cycle. The pulse characteristic could not be resolved during transit to the nozzle. Thus it was postulated that there might be a difference in response between a hot propellant gas and a cold gas. To ascertain whether this is true, the 5-in. x 15-in. motor was cold-flowed with helium and pulsed. Helium was chosen because the speed of sound is approximately the same, 3200 ft/sec, in helium and in propellant. The helium flow rate of 0.23 lb/sec was sufficient to cause choked flow at the nozzle and raise the chamber pressure to 100 psig using the same nozzle that was used with propellant. The gas was introduced at the head end of the motor containing an inert propellant with mechanical properties similar to those of PBAN 103. In both hot propellant gas and cold helium gas the pressure response to the black-powder pulse was nearly identical. In neither case could the wave be tracked beyond one cycle.

2. Geometrical Dampening Phenomena

In one of our early experiments using a rectangular slab motor, a core became malaligned, and as a result the center rectangular perforation was significantly out of alignment with the axis of the motor. It was decided to test the motor to ascertain whether this was a significant variable affecting either the initiation of axial mode instability or its characteristic response in the motor. Combustion was stable, even though pulsed considerably above the critical pressure predicted from our correlation for AP propellants.

It was postulated that stability was enhanced because the traveling wave, not intersecting normally with the reflecting surface (head end), lost energy after reflection. It was believed possible that certain other internal design factors might cause similar dampening. One proposed design was the introduction of a head end which was deliberately

out of alignment. An aluminum wedge 5 in. in diameter was attached to the pulse head in the 5-in. x 50-in. motor so as to tilt the face 30° from the perpendicular to the axis. The motor was loaded with a radial burning grain of PBAN 103 propellant, which has a critical threshold pressure of 600 psia. During the firing two significant observations were made. First, combustion was stable to 980 psia before the third pulse drove it unstable; during instability the wave form was extremely distorted and appeared to have a large harmonic content. Second, in all of our past testing with PBAN 103, an 80/20 AP/binder propellant, the instability invariably transitioned from axial to transverse (this normally caused higher chamber pressures and ruptured the nozzle safety bolts). In contrast, the slant head motor remained in the axial mode throughout burning.

The above experiments suggest strongly that energy losses at the ends, in particular the head end, contribute significantly to stability in both the axial and transverse modes. Heretofore the losses at the ends have been considered insignificant and have been neglected in most of the analyses of overall stability which have so far been published (e.g., the Hart-McClure theory). It is apparent that the viscous drag on the head end is probably a significant source of loss for transverse instability; in the case of traveling wave instability, our data (see next section) suggest that, in relation to the contact time of the shock front, an unexpectedly high rate of heat transfer occurs.

The influence of length to diameter ratio on stability is obviously explained by the fact that as the length decreased the end losses became more significant relative to the driving from the burning propellant.

3. Heat Transfer During Unstable Operation of a Motor

Heat transfer rates to the head end of a 5-in. x 40-in. motor operating in both the stable and unstable modes have been measured. During axial mode instability the heat transfer rate was approximately 660 BTU ft^{-2} sec^{-1}; during stable combustion it was 90 BTU ft^{-2} sec^{-1}. This high rate of heat transfer at the head end suggests that the inert head end serves as an energy sink and is as efficient as the nozzle in causing appreciable wave pressure losses. At this time it is postulated

that the primary mode of energy loss is by radiation. The thermal response of the cool head end is low compared to the frequency of the instability, and therefore the end is seeing an on-coming high temperature shock continuously. This same loss mechanism must operate at the nozzle end; however, it is modified by several factors.

The first factor to be considered at the nozzle end is the influence of the nozzle opening, which is a sink for mass and energy; the second is the two different surface environments interacting with the wave. In our representative test motor the outer annulus behaves somewhat like the head end except for the shape and emissivity (carbon versus steel at head end). The carbon nozzle would nevertheless present a rather cool reflection surface and absorption surface to thermal radiation from an advancing shock. The nozzle opening area is quite different in that the advancing pressure wave sees a high temperature shock front located in the nozzle throat. Radiative heat loss in this case would be expected to be minimized.

D. Nature of the Observed Traveling Wave Phenomena

This year attention has been focused on the behavior of traveling waves in the combustion chamber, and especially upon further interpretation of the available data. Typical experimental behavior is shown in Fig. 13 for PBAN 319 propellant in an 82-in. slab motor operating at a mean pressure of 1260 psia. The important point to be noted is that the head-end pressure pulse is approximately twice as large as the pulses measured at the one-quarter and three-quarter length stations. The aft-end pulse is somewhat smaller than the head-end pulse, presumably because this pressure is measured 4 in. upstream of the nozzle. A possible additional contributing factor may be energy loss upon reflection from the open nozzle.

From a phenomenological point of view, the behavior illustrated by the pressure traces of Fig. 13 can be explained by the presence of a constant strength shock-expansion process which is traveling back and forth in the motor. The passage of the shock wave past any point induces a particle velocity behind it in the direction of travel of the shock, as well as pressure and temperature jumps. In order to satisfy the

continuity equation, an expansion process which reduces the induced velocity to zero must form behind the shock wave, as shown schematically in Fig. 14. Since the expansion process is isentropic, the local velocity of the expansion field will be the local speed of sound which decreases with increasing distance behind the shock wave. Thus the extent of the expansion process will lengthen as wave travel proceeds down the chamber.

When the shock wave reflects from the end of the chamber, the measured perturbation amplitude doubles because the shock wave will maintain the same pressure change across itself, whereas the pressure in front of the reflected shock is the pressure which was behind the incident shock. A correspondingly strong expansion process will follow the reflected shock back down the passage toward the oncoming expansion process which was following the incident shock. This incoming expansion process reduces the strength of both the reflected shock and its trailing expansion process down to the strengths of the original process and the chain of events is repeated in the opposite direction. This complicated turn-around process occurs in a very short physical distance, making the details very difficult to obtain experimentally.

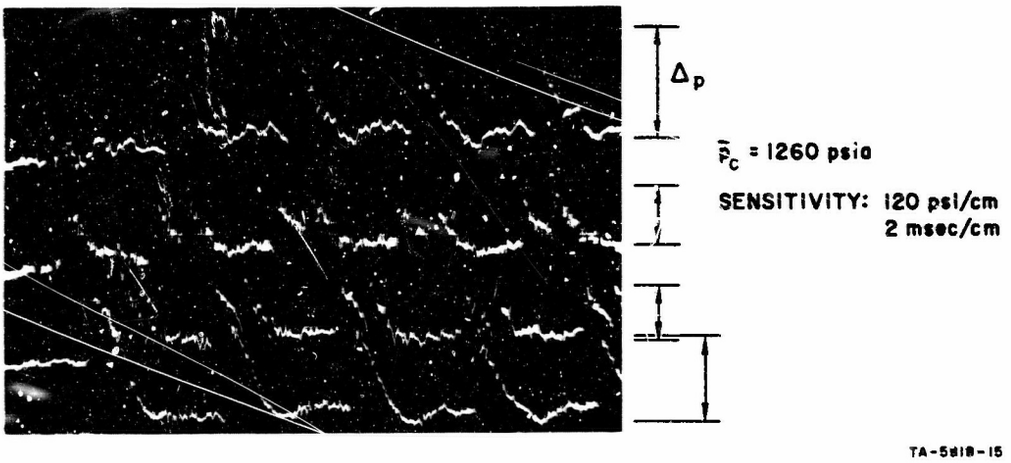

FIG. 13 TRAVELING WAVE INSTABILITY IN A SLAB BURNER

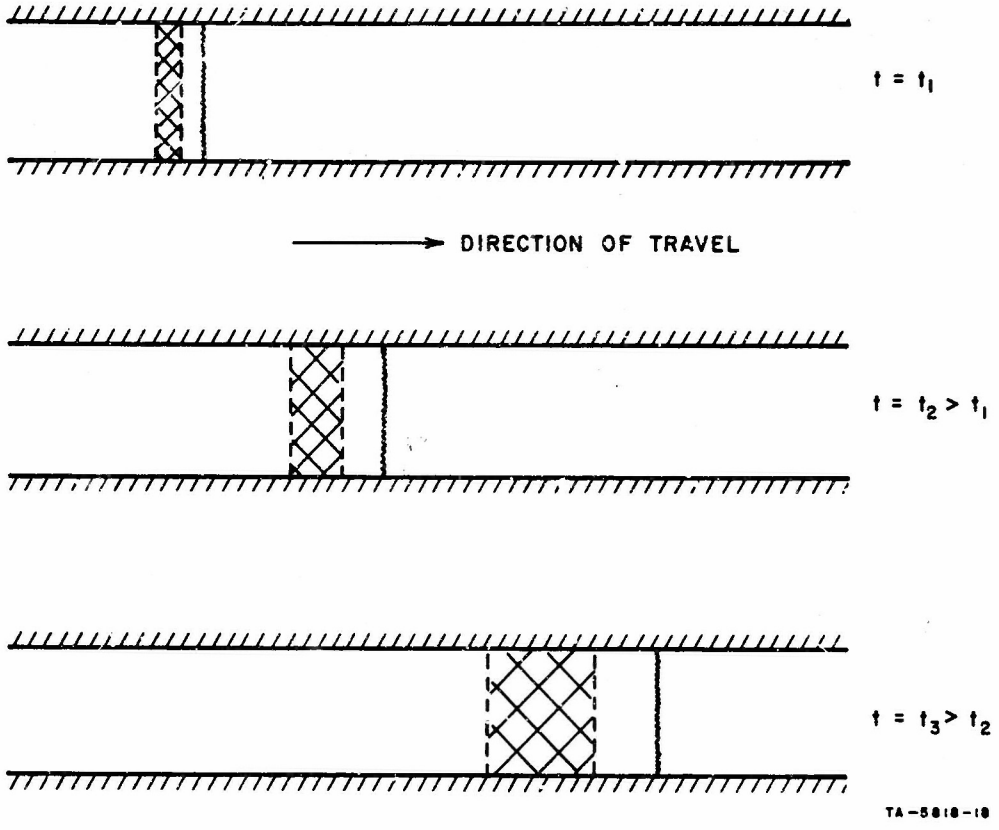

FIG. 14 SCHEMATIC EVOLUTION OF THE SHOCK-EXPANSION PROCESS DURING LONGITUDINAL INSTABILITY

This physical reasoning is borne out by further examination of Fig. 13. Not only does pressure-doubling occur at the ends, but the wave velocity along the chamber is nearly constant, since a comparison of the data at the quarter-length point with that at the head-end shows that about one-quarter of the total wave travel time is used over the first quarter of the motor. A constant wave velocity implies a constant wave strength; within the accuracy of the traces, the strengths at the one-quarter and three-quarter points are the same.

The final strength (and therefore velocity) of the wave will be determined by the balance between the energy imput process and the dissipation process at the walls and by the coupling between the passage

of the wave and the primary combustion process. This latter coupling is discussed in detail in a later section. A possible mechanism for the local input of energy into the traveling wave is the heat release from gas-phase reactions which are induced by the temperature jump across the shock wave.

The pressure difference across a shock wave is related to the Mach number and the pressure ahead of the shock by

$$\frac{\Delta p}{p_1} = \frac{2\gamma}{\gamma + 1} (M^2 - 1) \qquad (1)$$

Data to support the hypothesis that the finite amplitude wave is a pure shock (P.S.) rather than a Chapman-Jouget (C-J) detonation is shown in Table IV. Using the pressure data from experimental rocket motors, the Mach number appropriate to either type of wave can be computed. With motor length and periodic frequency known, it is then possible to calculate the velocity of sound. This experimentally derived value can then be compared with that predicted from thermochemical data for the propellants.

TABLE IV

COMPARISON OF THEORETICAL AND EXPERIMENTALLY DERIVED SOUND VELOCITIES

Propellant and Motor Type	PBAN 103 Slab	PBAN 103 Tubular	PBAN 104 Tubular
Chamber pressure - psia	1,230	1,200	565
Pressure ratio	0.0813	0.1875	0.169
Mach number (C-J)	1.08	1.18	1.142
Mach number (P.S.)	1.04	1.09	1.078
Motor length - inches	82	82	82
Wave recurrence frequency, cps	236	242	244
Velocity of sound, experimental (C-J), fps	2,985	2,810	2,920
Velocity of sound, experimental (P.S.), fps	3,100	3,035	3,085
Velocity of sound,* thermochemical, fps	3,218	3,218	3,129

*Computed at 1,000 psia.

In examining Table IV, it will be noted that the velocity of sound calculated on the basis of a pure shock wave is much closer to the thermochemically derived value. The discrepancy in this case can most probably be attributed to the overall combustion efficiency being about 95-97%; this is a reasonable value on the basis of specific impulse measurements. In the case of a Chapman-Jouget wave, the required combustion efficiency would be of the order of 85%; this is unreasonably low and cannot be substantiated by past experience. Since the dissipation might be expected to be less in a tubular burner than in a slab burner, a stronger shock wave would be expected in a tubular burner. That this is indeed the case is shown Table IV.

To summarize, traveling wave data obtained in a slab burner support the concept of the instability being a constant strength shock wave which may be partially supported by an energy input from induced gas phase reactions behind the shock. More important is the coupling between the wave process and the main combustion process which is discussed in detail below.

Head-end pressure measurements obtained in tubular motors with five different propellants are shown in Fig. 15. Two traces are shown for each propellant, the lower one of which has been filtered to remove the organ pipe oscillation in the small cylindrical chamber ahead of the transducer. Results are given in Table V, along with propellant compositions.

The wave amplitude (see Table V), computed as half the head-end pressure pulse for reasons discussed above, is relatively constant for all the propellants considered, being about $\Delta p/\bar{p} = 0.17$. The variations which do occur undoubtedly depend more upon the ratio of the mean pressure to the threshold pressure for instability than upon compositional factors in these similar AP-based propellants.

TABLE V

TUBULAR MOTOR INSTABILITY DATA

Propellant	Composition	Motor Length (inches)	Wave Amplitude ($\Delta p/\bar{p}$)	Wave Frequency (cps)
PBAN 103	24% ground* } NH_4ClO_4 56% unground } 20% PBAN	40	0.185	600
PBAN 104	22.5% ground* } NH_4ClO_4 56% unground } 20% PBAN 1.5% LiF	82	0.169	244
PBAN 244	27% ground* } NH_4ClO_4 52% unground } 20% PBAN 1% LiF	40	0.163	500
PBAN 284	20% - 20μ 20% - 600μ } NH_4ClO_4 39.5% unground } 20% PBAN 0.5% $SrCO_3$	40	0.138	513
PBAN 319	22% - 20μ 22% - 600μ } NH_4ClO_4 34% unground } 17% PBAN 5% Al	82	0.184	250

*Average particle diameter of 10 μ.

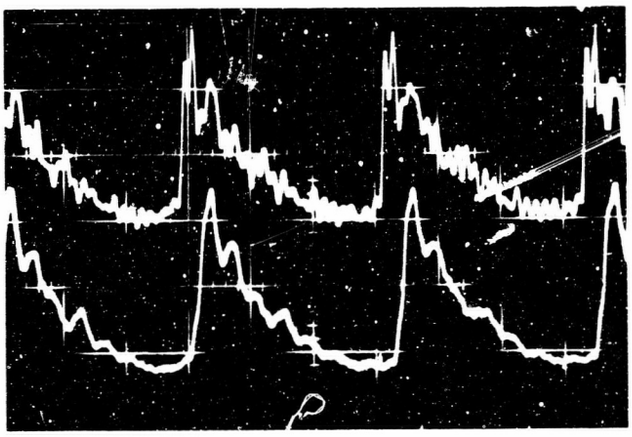

PBAN 103

$\bar{p}_c$ = 915 psia

SENSITIVITY: 120 psi/cm
0.5 msec/cm

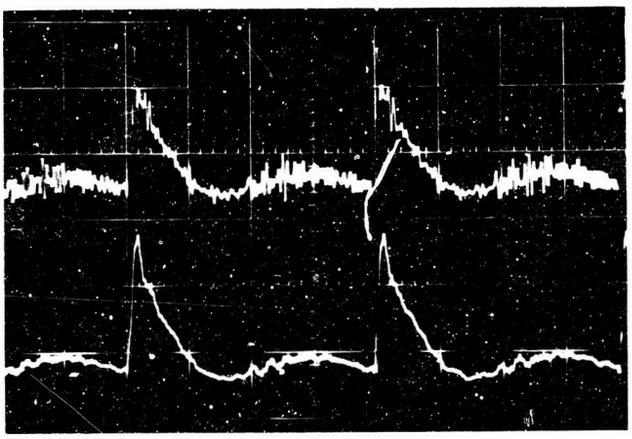

PBAN 104

$\bar{p}_c$ = 565 psia

SENSITIVITY: 80 psi/cm
1 msec/cm

TA-5818-16

FIG. 15 HEAD-END PRESSURE TRANSIENTS DURING TRAVELING WAVE INSTABILITY IN A TUBULAR BURNER

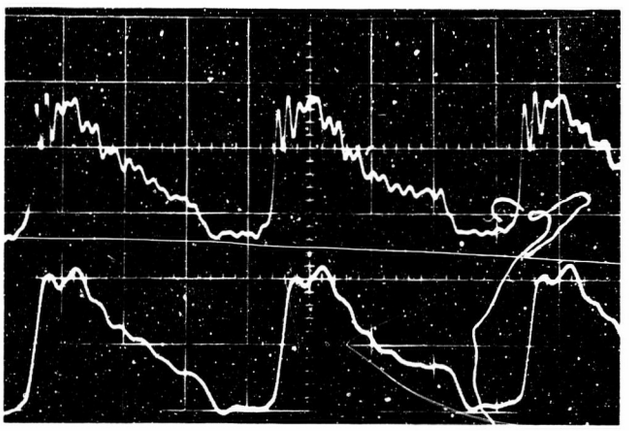

PBAN 244

$\bar{P}_c$ = 410 psia

SENSITIVITY: 60 psi/cm
0.5 msec/cm

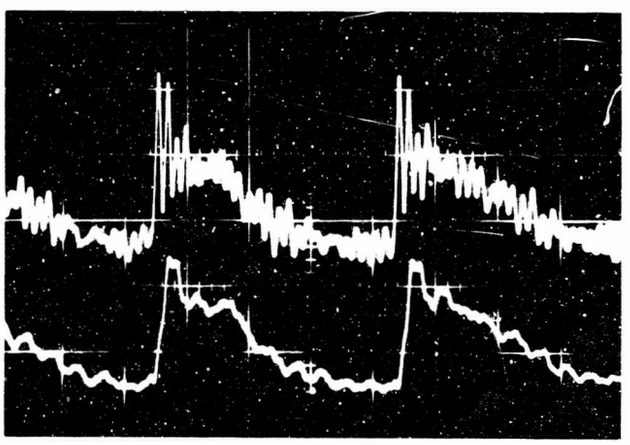

PBAN 284

$\bar{P}_c$ = 635 psia

SENSITIVITY: 80 psi/cm
0.5 msec/cm

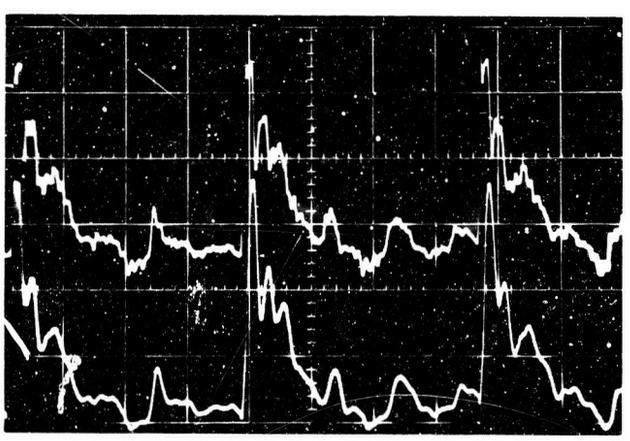

PBAN 319

$\bar{P}_c$ = 1215 psia

SENSITIVITY: 120 psi/cm
1 msec/cm

TA-5818-17

FIG. 15 Concluded

III THEORETICAL STUDIES

The role of the combustion process in determining the stability of the chamber can be described in terms of the admittance of the propellant surface, which depends directly on the propellant response function.[11] The response function is a property only of the combustion process, and the objective of much theoretical[11] and experimental[12] effort has been to evaluate this parameter. Most of the theoretical attempts to relate the response function to thermal and chemical processes comprising the combustion mechanism[3,13-15] have been quite similar, differing mainly in details of the mathematical formulation of the combustion model. These analyses have been concerned only with the pressure response of the propellant; i.e., velocity coupling has been neglected. Until very recently they have employed combustion models that assume all heat release to occur in the gas phase, with no exothermic (or endothermic) surface reactions.[3,13,14] Such surface reactions have been included by Friedly and Petersen,[15] but the complexity of their numerical analysis masked the natural relationships which exist among the governing parameters, so that a considerably more illuminating presentation is possible. Also, the considerable complexity of the treatment is rather inconsistent with the order-of-magnitude accuracy to which relevant thermochemical parameters can be measured or estimated. Culick[16] has provided a much less complex treatment, which accounts for surface exotherms or endotherms, by employing a highly simplified description of the gas-phase reactions. Unfortunately, this approach may introduce an unacceptable simplification, for in some cases it leads to anomalous results such as a negative response function. In addition both of these analyses combine all surface-coupled reactions into a single step, neglecting the possibility of reactions which are separated from the pyrolysis step by intermediate macroscopic mixing.

During this program we have developed a theoretical analysis of the solid propellant response function based on a combustion model that specifically includes surface-coupled exothermic or endothermic reactions. Surface-coupled reactions are here defined as those reactions which are

thermally coupled to the temperature response of the solid propellant through the associated kinetic rate equations. Such reactions occur in a narrow zone at the gas-solid interface and are not necessarily strictly confined to the solid phase; for example, they may be heterogeneous in character. In an effort to overcome the objections noted above, a different approach, in terms of both the kinetics and the mathematical formulation, has been taken. We believe this analysis provides a clearer picture of the highly significant role of surface-coupled reactions in unstable combustion. A consistent and potentially important interpretation of traveling-wave axial-mode instability phenomena is now emerging from the theory.

Our goal has been to consider the most important features of the combustion mechanism in a combustion model that is reasonably realistic, yet mathematically tractable and capable of clear interpretation. A number of investigators have employed empirical steady-state burning rate expressions, or the equivalent, to achieve very simple analyses of transient solid propellant combustion phenomena. Such analyses are really quasi-steady in nature and limited to very low frequency phenomena. They are not valid for instability phenomena of practical interest. Others have carried out enormously complex mathematical analyses that are completely inconsistent with our currently rather primitive understanding of the detailed structure of the combustion process. The results are usually of questionable value, as well as inaccessible. Among the previous investigators, Denison and Baum[3] seem to have avoided these undesirable extremes more successfully than most, although their combustion model fails to account for surface-coupled energetic reactions.

Accordingly, the present analysis is accomplished by performing a mathematical transformation of the treatment by Denison and Baum to make it applicable to a new model, in which surface-coupled reactions are considered. Thus, from a mathematical viewpoint the present analysis is formally identical to that of Denison and Baum, but describes the behavior of a more realistic and more general combustion model. In the absence of surface-coupled reactions, the present treatment reduces to Denison and Baum's.

The Appendix of this report contains a relatively complete presentation of the theoretical analysis developed during this program, including a review of the assumptions and basic concepts underlying the mathematical formulation of the combustion model. In the following sections of the text the main conclusions derived from this analysis are discussed, and our current theoretical interpretation of experimental observations during this program is summarized.

A. Implications of the Theoretical Analysis

The theoretical model presented in the Appendix is based on a mathematical transformation of the previous work of Denison and Baum,[3] who considered the case of zero surface heat release. Their solution showed that a given propellant can be characterized in terms of three parameters: A, which relates to the surface decomposition kinetics; α_0, which relates to the gas-phase kinetics, (the subscript zero refers to zero heat release) and ν, the steady-state pressure exponent. The physical meaning of these parameters is discussed in detail in the Appendix.

Denison and Baum's mathematical solution culminated in a stability map in the $A\text{-}1/\alpha_0$ plane which contained two limit lines--one separating a stable region from a region of unstable oscillatory response with an exponential envelope (termed the "self-excited" mode by Denison and Baum), and one separating this latter region from a region of purely exponential unstable response. Only the first of these limit lines has any physical meaning, since all propellants which are not incipiently unstable must lie in the stable region; only its behavior will be considered here.

Figure 16 shows the Denison-Baum limit line as the heavy line. The stable region lies to the left of the limit line. When surface heat release is present, an additional parameter θ_s, which is related to the proportion of surface-coupled heat release, enters the solution. The mathematical transformation discussed in the Appendix allows the immediate prediction of the shift in the limit line which is induced by surface reactions. In the $A\text{-}1/\alpha_0$ coordinate system it is possible to directly illustrate the effect of surface heat release on the extent of the stable

region. It is important to understand, however, that the transformation given in the Appendix collapses all of the limit lines into the "universal" Denison-Baum line in the A-$1/\alpha$ coordinate system; i.e., the heavy line of Fig. 16 becomes a universal curve when the abscissa is identified as $1/\alpha$ rather than $1/\alpha_0$.

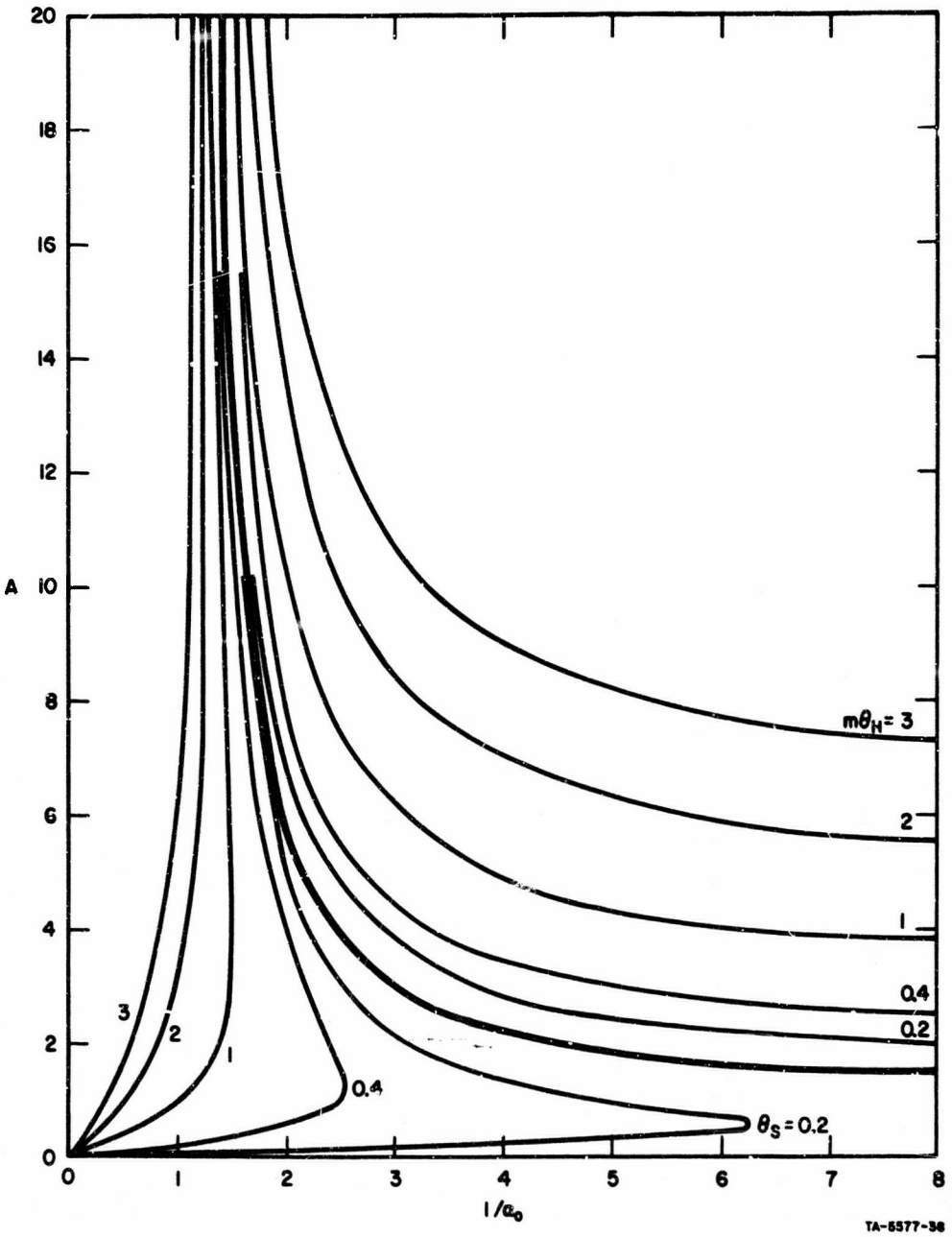

FIG. 16 STABILITY LIMITS FOR THE SELF-EXCITED MODE

The curves which lie below the Denison-Baum line in Fig. 16 correspond to the composite propellant heat release described in the Appendix. It can be seen that a relatively small proportion of surface-coupled heat release can profoundly decrease the region of stable operation. For fixed values of A, the effect becomes more pronounced as A decreases. The curves which lie above the Denison-Baum line correspond to the double-base propellant model for which $\theta_s = m\theta_H$. In this case the effect of surface-coupled heat release is found to be stabilizing, in agreement with the work of Soviet investigators.[17]

Close to the limit line, but in the stable region, it is possible to obtain a large amplitude response to a forcing function. Such a response will have a preferred frequency which is near the unbounded oscillatory frequency; it is termed the steady oscillatory response by Denison and Baum. The response of the surface mass addition rate to a sinusoidal forcing pressure fluctuation was derived by Denison and Baum[3] and can be stated in our notation as

$$\frac{1}{\nu}\frac{\tilde{m}}{\tilde{p}} = \frac{A\alpha}{\sqrt{a^2+b^2}} \frac{\omega K}{\bar{r}^{-2}} \sin(\omega t - \Phi) \tag{1}$$

where the phase angle Φ is given by

$$\Phi = \tan^{-1}(b/a) + \pi/2 \tag{2}$$

and where

$$a = A(1 + \lambda_r) - \frac{\omega K}{\bar{r}^{-2}}\lambda_i \; ; \; b = \frac{\omega K}{\bar{r}^{-2}}(\lambda_r + q) + A\lambda_i$$

$$\lambda_i = -\frac{1}{2}\left[\frac{-1 + (1 + 16\omega^2 K^2/\bar{r}^{-4})^{1/2}}{2}\right]^{1/2}$$

$$\lambda_r = -\frac{1}{2}\left\{1 + \left[\frac{1 + (1 + 16\omega^2 K^2/\bar{r}^{-4})^{1/2}}{2}\right]^{1/2}\right\}$$

$$q = 1 + A(1 - \alpha)$$

Frequency response curves for selected values of A and α are shown in Figs. 17 and 18. These curves correspond to the universal representation of the limit line which is obtained from the transformation. Figure 17 shows the absolute value of the ratio of the mass flow perturbation from the surface to the pressure perturbation, normalized by the steady-state pressure exponent ν. Such a normalization is required to obtain a universal representation of the response function. Figure 18 shows the real part of the mass flux/pressure perturbation ratio; i.e., the component of the response function that is in phase with the pressure perturbation. It is this quantity which enters any general stability analysis.

A family of curves is shown for A = 10. A decreasing value of α corresponds to horizontal movement to the left away from the universal limit line of Fig. 16. Near the limit line very small changes in α cause large changes in the amplitude of the response. This demonstrates the importance of the location of the limit line for any given propellant. At values of α near the limit line the real part of the response shown in Fig. 18 has a narrower peak than the absolute response shown in Fig. 17, but the peak amplitudes are nearly the same, reflecting the nearly zero phase shift which occurs near the peak. (The real part of the response is not shown for the limiting value of α, since only in this case does the phase angle exceed 90 degrees, giving rise to a spurious negative real part. In practice, operation on the limit line itself can never be attained.) As the amplitude of the response decreases with increasing α, the response curves broaden and the real part becomes more nearly like the absolute response. Also, the value of the frequency at which resonance occurs shifts only slightly with α at a fixed value of A.

For an illustrative example to clarify the importance of surface-coupled reactions, consider a composite propellant for which

$$T_f = 2300^\circ K,\ T_w = 1000^\circ K,\quad T_o = 300^\circ K$$

$$E_f = 27.5 \text{ kcal},\ E_w = 30 \text{ kcal}$$

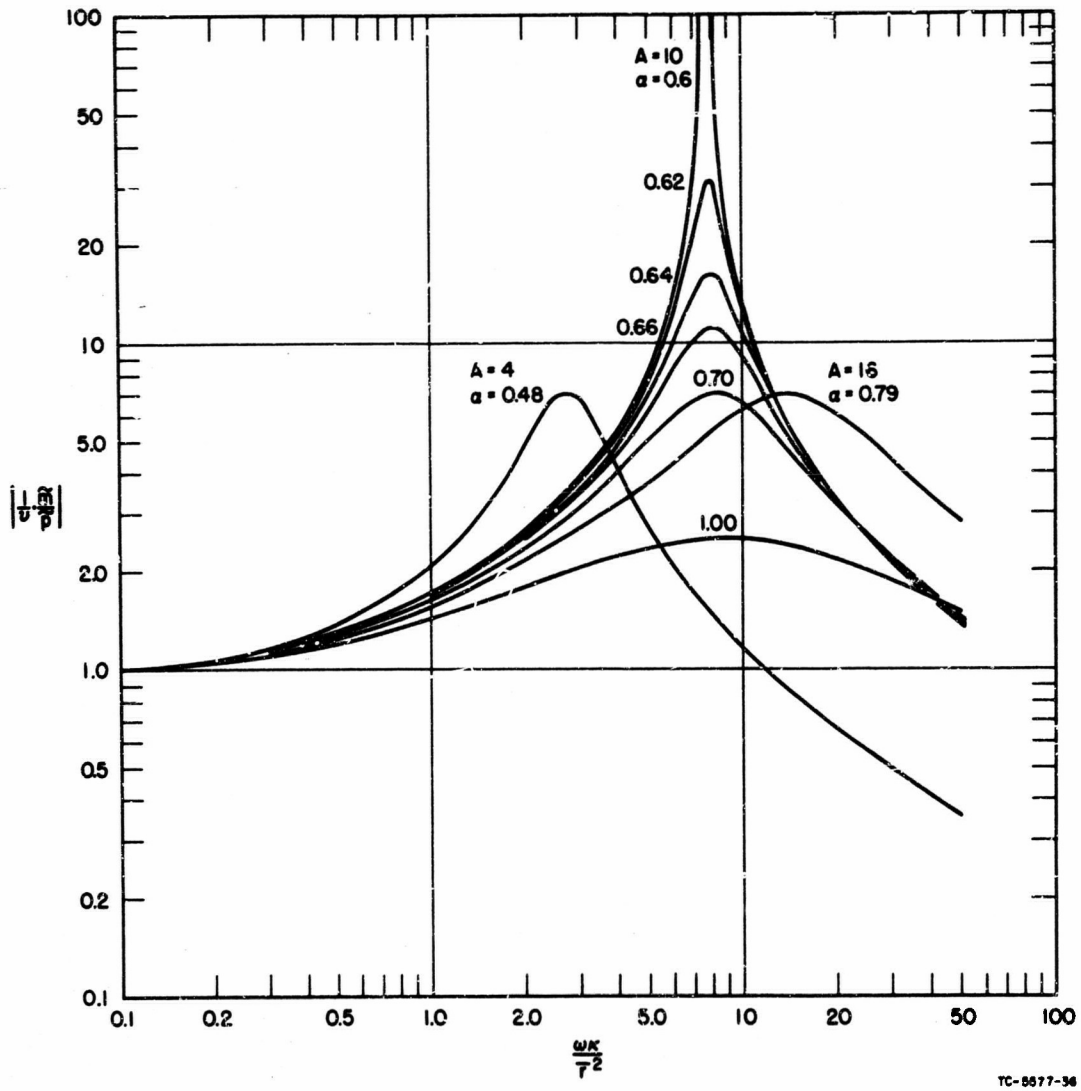

FIG. 7 ABSOLUTE VALUE OF THE RESPONSE FUNCTION IN THE STEADY OSCILLATORY MODE

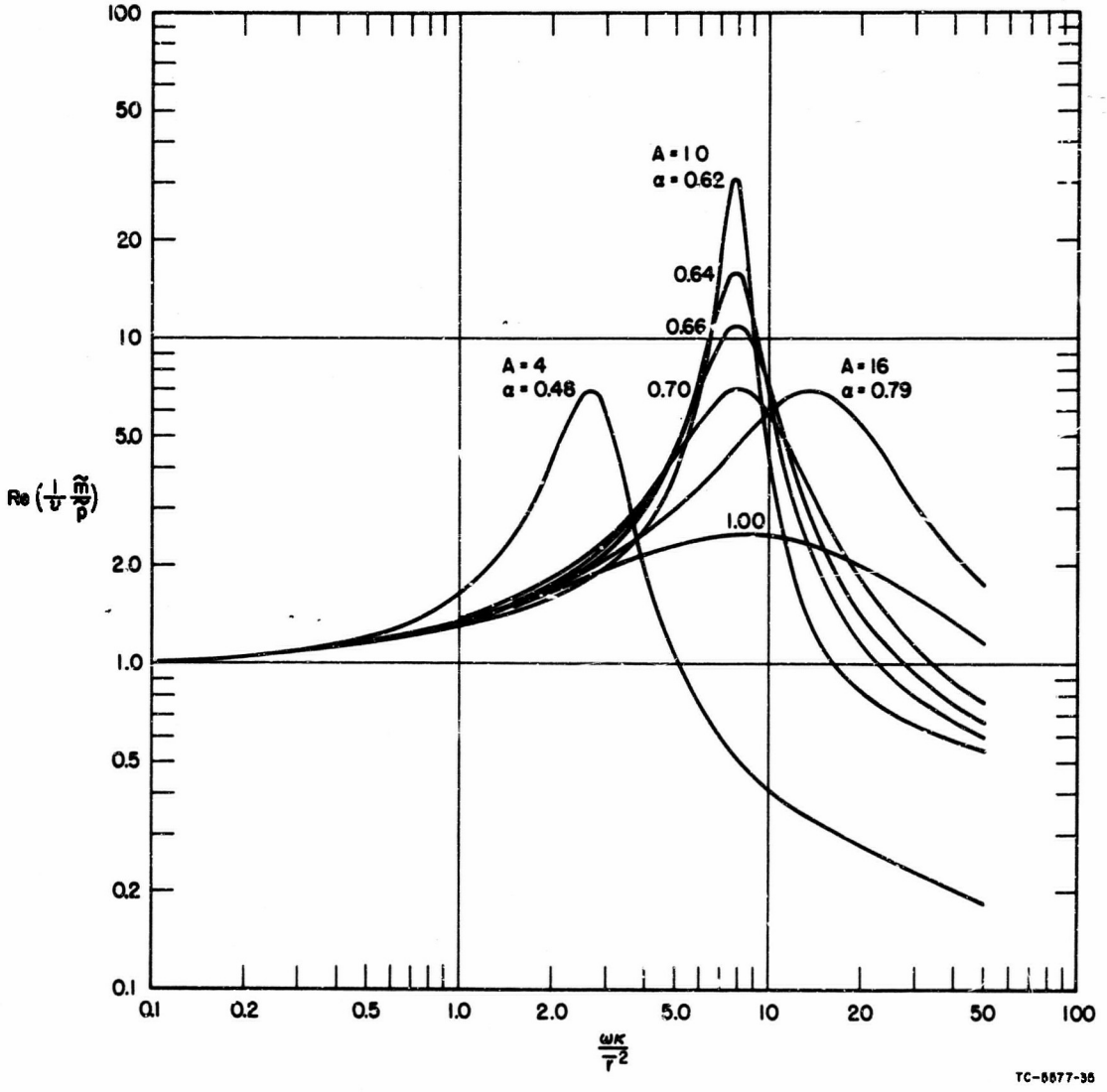

FIG. 18 REAL PART OF THE RESPONSE FUNCTION IN THE STEADY OSCILLATORY MODE

These choices give a value of $\alpha_0 = 0.66$, and the amplitude response is given by the corresponding curves of Figs. 17 and 18 when there is no surface-coupled heat release ($\theta_s = 0$). In contrast, if $\theta_s = 0.4$ (roughly 4 percent of the total heat release at the surface), Eq. 12 in the Appendix gives $\alpha = 0.62$ and Figs. 17 and 18 show that the amplitude of the response is nearly tripled. This demonstrates the strong influence that can be exerted by a very small surface heat release and helps to explain the sharp experimental demarcation between stable and unstable operation which was obtained previously.[2]

Also shown in Figs. 17 and 18 are response curves for A = 4 and 16 whose amplitudes are equal to that of the A = 10, $\alpha = 0.70$ case. As the value of A increases, the response broadens markedly (note the logarithmic scale). This implies that propellants having a high activation energy of decomposition will be susceptible to random forcing functions over a much wider frequency band than those having lower activation energies. Since the limit lines on Fig. 16 become more nearly vertical as A increases, the value of α corresponding to a constant amplitude response changes more and more slowly with increasing A. Finally, in connection with Figs. 17 and 18 it is important to note that the solution approaches the correct limits at large and small values of the frequency; i.e., as $\omega \to \infty$, $\left| \tilde{m}/\nu\tilde{p} \right| \to 0$ and as $\omega \to 0$, $\left| \tilde{m}/\nu\tilde{p} \right| \to 1$; the real part also satisfies these limits.

Figure 19 shows the phase angle behavior for the A = 10 family of freguency response curves. For all values of α the rate of change of phase angle at $\omega = 0$ is the same and the return to zero phase angle occurs at the same value of $\omega K/r^{-2}$. The peak in the response (see Fig. 17 or 18) shifts across this value of nondimensional frequency in the direction of increasing ω as α increases, and always occurs near it. The total swing in the phase angle decreases as α increases, as implied previously in connection with the fact that the real response approaches the absolute response as α becomes larger.

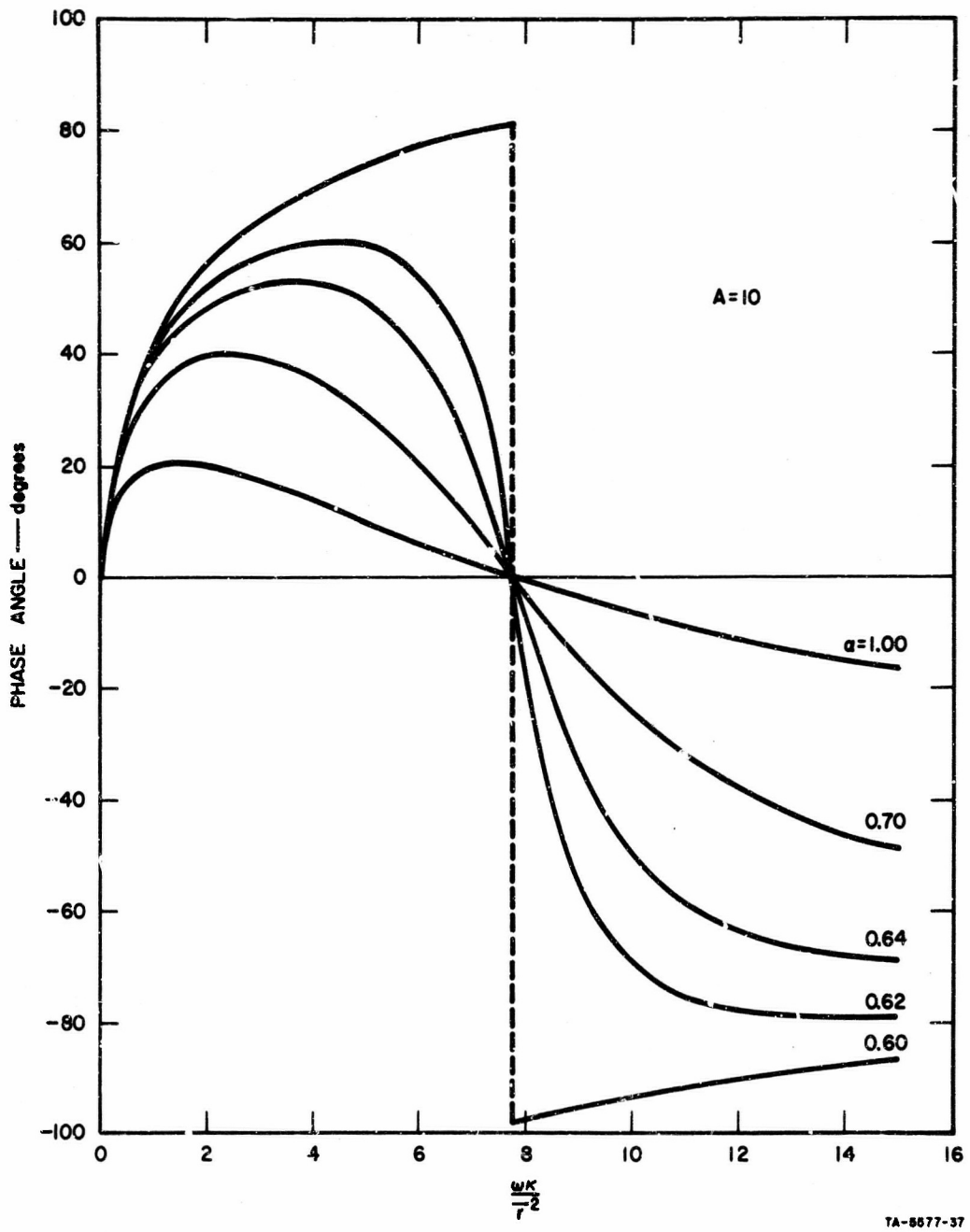

FIG. 19 PHASE RELATION BETWEEN MASS FLUX PERTURBATION AND PRESSURE PERTURBATION IN THE STEADY OSCILLATORY MODE

It is important to remember that the above analysis is limited to an upper frequency of a few thousand cycles per second, because the relaxation processes in the gas phase have been completely neglected. For the A = 10 case where resonance occurred near $\omega K/\bar{r}^2 = 8$, the corresponding frequency would be 51 cps if $\bar{r}$ = 0.1 in./sec and 1270 cps if $\bar{r}$ = 0.5 in./sec, using K = 2.5 X 10^{-4} in.^{2}/sec. These values are within the regime of validity for the analysis, but with substantially higher values of A, for example, the results might be restricted to burning rates somewhat lower than 0.5 in./sec.

B. Theoretical Explanation of Observed Frequency Characteristics

The experiments which have been carried out have confirmed in broad outline the model discussed above. As has been well-documented previously in this program,[18] axial mode combustion instability arises when a pressure disturbance is able to overcome the damping which is present in the chamber and develops into a traveling wave reflecting back and forth between the ends of the chamber. Typical experimental behavior is shown in Fig. 20 for PBAN 319 propellant in a slab motor operating at a mean pressure of 1260 psia. The head-end and aft-end pressure pulses are nearly equal in magnitude and approximately twice as large as the pulses measured at the one-quarter and three-quarter length stations. The aft-end pulse is slightly smaller than the head-end pulse, presumably because of some energy loss upon reflection from the open nozzle. The velocity of wave travel corresponds to a Mach number of about 1.2.

The final strength (and therefore velocity) of the wave will be determined by the balance between the energy input process and the dissipation process at the walls and by the coupling between the passage of the wave and the primary combustion process. A possible mechanism for the local input of energy into the traveling wave is the heat release from completion of gas-phase reactions at the wall induced by the temperature jump across the shock wave. It conservatively appears that less than 2 percent of the available propellant energy is needed for direct input to the wave.[18]

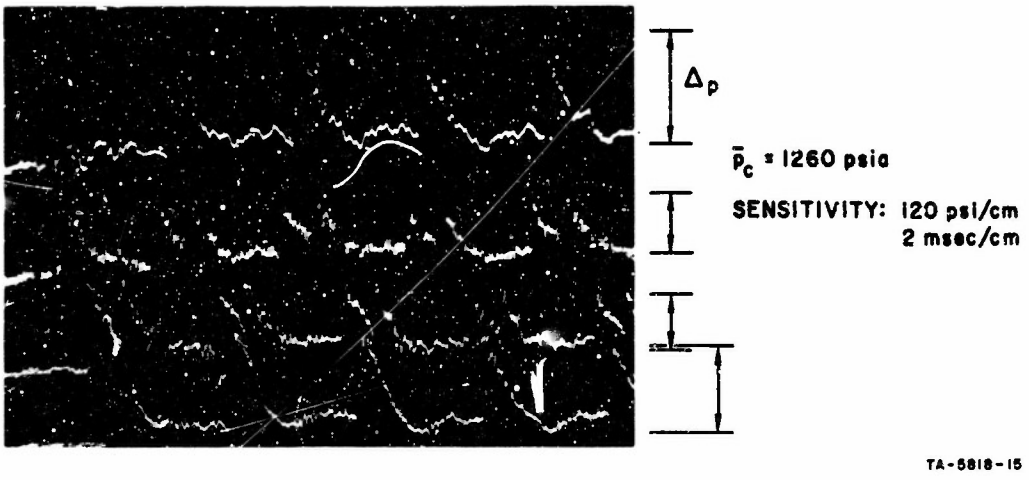

FIG. 20 TRAVELING WAVE INSTABILITY IN A SLAB BURNER

This observation leads to a very important conclusion; it is unlikely that the appearance of axial-mode instability is governed primarily by the amount of energy feedback from the combustion process to the traveling wave, since so little energy is needed to support the wave. Of course, the energy flux magnitude does play a significant role, particularly in a motor with a high damping factor, or high losses. However, it is likely that a more important factor in determining the axial-mode stability characteristics of a solid rocket motor is the phase relationship between the energy feedback at any given point on the propellant, and the passage of the wave over that point. In other words, if the energy feedback (or mass-flux perturbation at the surface, which is essentially equivalent) is locally in phase with the passing shock wave over most of the burning surface. the shock wave will be reinforced and instability will result. If the two events are locally out of phase over most of the length of the grain, the shock wave will decay and stable combustion will be achieved. This phase relationship is determined by the combustion chamber length and by the frequency response characteristics of the combustion mechanism.

As the shock wave travels axially back and forth in the combustion chamber, it creates an oscillatory pressure disturbance at every point on the propellant surface. The frequency of this disturbance at any given axial position corresponds to the number of times per second that the wave passes this position. In general, there are two distinct frequencies associated with any given axial position. One of these corresponds to the time required for a shock wave traveling toward the right to be reflected from the right end of the chamber and return to the reference point. The other frequency corresponds to the time for a wave traveling toward the left end to be reflected and return to the same point. At the ends of the chamber only one of these frequencies pertains (i.e., the other is infinite); at the center they are equal, of course. From a brief consideration of this phenomenon one can readily see that the pulse frequency at the center of the chamber is exactly twice that at the ends. At intermediate stations the propellant is subjected to a train of pulse pairs. For example, at one-quarter and three-quarter positions the separation between pairs corresponds to a recurrence frequency of two-thirds of that at the center, while the spacing between two pulses in a pair corresponds to a frequency of twice that at the center. The band of frequencies encountered is dependent on the motor length and the motor surface is dependent on the net driving and damping of the wave train.

Pulse frequencies encountered in experiments performed during this program[3] are shown in Table VI.

For the 23-, 40-, and 82-in. motors, frequencies were measured at the head-end pressure transducer. As mentioned earlier, these frequencies are produced by a traveling shock wave moving at $M \cong 1.2$ back and forth in the chamber. Ordinarily, pulses introduced in the 15-in. motor were found to decay, i.e., with most propellants this motor could not be driven to unstable combustion. The frequencies shown in Table VI for this motor are the calculated characteristic frequencies based on a traveling shock wave with $M = 1.2$.

TABLE VI

FREQUENCY OF PRESSURE PULSE, cps

Length of Chamber, in.	End	Axial Position		Center
		1/4 L	3/4 L	
15	1240	1660	4960	2480
23	803	1070	3212	1606
40	435	620	1860	930
82	238	318	952	476

In order to compare these values with the theoretical response curves discussed earlier, it is necessary to assign approximate values to the thermochemical parameters that characterize the propellants. For most composite propellants it is reasonable to assume that the activation energy for surface decomposition is $E \approx 30$ kcal. The surface temperature T_w is approximately 800°K, and the gas-phase flame temperature is $T_f \approx 2500°K$. The activation energy for the gas-phase flame usually is $E_f \approx 20$ kcal and the overall effective order of reaction n is about 2. The parameters for a very wide range of propellants, including those that have been investigated experimentally in this program, almost certainly fall within 20% of these values. If, additionally, approximately 10 percent of the heat release occurs near the surface so that $\theta_s = 0.1$, a typical composite propellant is characterized in Fig. 17 or 18 by the coordinates $A \sim 10$, $\alpha \sim 0.7$. It follows that the peak amplitude ratio is about 7 for such propellants, and the resonant frequency of the combustion mechanism corresponds to $K\omega/\bar{r}^2 \sim 8$, or $f \sim 8\bar{r}^2/2\pi K$. The maximum deviation from this frequency for which there is a significant burning-rate amplification is about:

$$\Delta f \cong \pm 3\bar{r}^2/2\pi K$$

A typical thermal diffusivity for solid propellants is $K \approx 2.3 \times 10^{-4}$ in^2/sec. Accordingly, the approximate frequency range in which the combustion mechanism tends to amplify a pressure oscillation is as indicated in Table VII. The frequency given in the table is the approximate resonance frequency, or point of maximum amplitude, and the tolerance figures indicate the approximate range in which a degree of amplification is present.

TABLE VII

APPROXIMATE RESONANT-FREQUENCY RANGE FOR A TYPICAL COMPOSITE PROPELLANT ACCORDING TO THEORETICAL COMBUSTION MODEL

$\bar{r}$ (in./sec)	f (cps)
0.1	~53 ± 20
0.2	~220 ± 80
0.3	~500 ± 190
0.4	~890 ± 330
0.5	~1380 ± 520

It is reasonable to assume that axial-mode combustion instability may arise in a solid rocket chamber whenever an appreciable portion of the grain length is subjected to pressure oscillations near the resonance frequency of the combustion mechanism. On this basis a comparison of Tables VI and VII affords some interesting conclusions.

In a 15-in. chamber, only a very high burning rate propellant should be susceptible to axial-mode instability. With a 0.5-in./sec burning rate, only the portion of the propellant near the ends of the chamber can experience pressure oscillations in the resonance range. With lower burning rates, no part of the combustion surface is in resonance with the waves. Thus, with propellants in the normal burning rate range the theory predicts that combustion instability should be difficult to initiate (or rarely experienced) in a 15-in. chamber. This agrees with our experimental observations.

Instability is much more likely in the 23-in. and 40-in. chambers. In the former, propellants with burning rates of 0.35 to 0.45 in./sec should be particularly susceptible to instability. The corresponding range in the 40-in. chamber is about 0.2 to 0.4 in./sec. The stability characteristics of a number of propellants have been thoroughly documented experimentally in a 40-in. chamber during this program.[2] The results are shown in Fig. 21. It is apparent that the burning rates of the propellants that encountered instability fell in the range 0.1 to 0.3 in./sec. Though this range is somewhat lower than that predicted theoretically, the agreement is well within the tolerances imposed by uncertainties in evaluating the thermochemical constants of the propellant. The theoretically predicted resonance-frequency bounds offer a plausible explanation for the fact that the high burning rate AP/KP propellant was stable, whereas the other one was not. They may also explain why the KP, LiP, and AN propellants were stable, as all these have resonance frequencies well outside the wave frequencies typical of a 40-in. motor. However, there is also another factor that may be significant here--the value of θ_s which determines the amplitude of the burning rate response. This factor certainly appears to be important relative to the opposite behavior of the AN/KP and AN/AP propellants, which should have similar resonance frequencies.

In the 82-in. motor it was found experimentally that the shock wave traveled from end to end of the motor, with the frequencies shown in Table VI, only during the first 100 msec after the initiating pulse. In every case the motor failed to sustain such a mode beyond this initial period. Instead, a transition to a double mode, or essentially the first harmonic, always occurred. In this case there were two traveling shock waves in the motor, each traveling through a 41-in. section and reflecting off the other wave at the center. Thus, the 82-in. motor always undergoes a transition to an axial instability mode that exhibits the same frequency range as that shown for a 40-in. motor in Table VI. This is precisely what one would expect for this propellant (PBAN 103, $\bar{r} \sim 0.25$-0.3 in./sec) from the theoretical analysis of Table VII. The fundamental mode of the 82-in. motor corresponds to a frequency range (Table VI) that is somewhat below the resonance frequency-response range of the propellant. However,

the double-wave mode, which corresponds to the frequencies of a 40-in. motor (Table VI), is right in the resonance range, as has already been shown. Thus the transition to this mode in the longer motor is entirely consistent with the theoretical predictions.

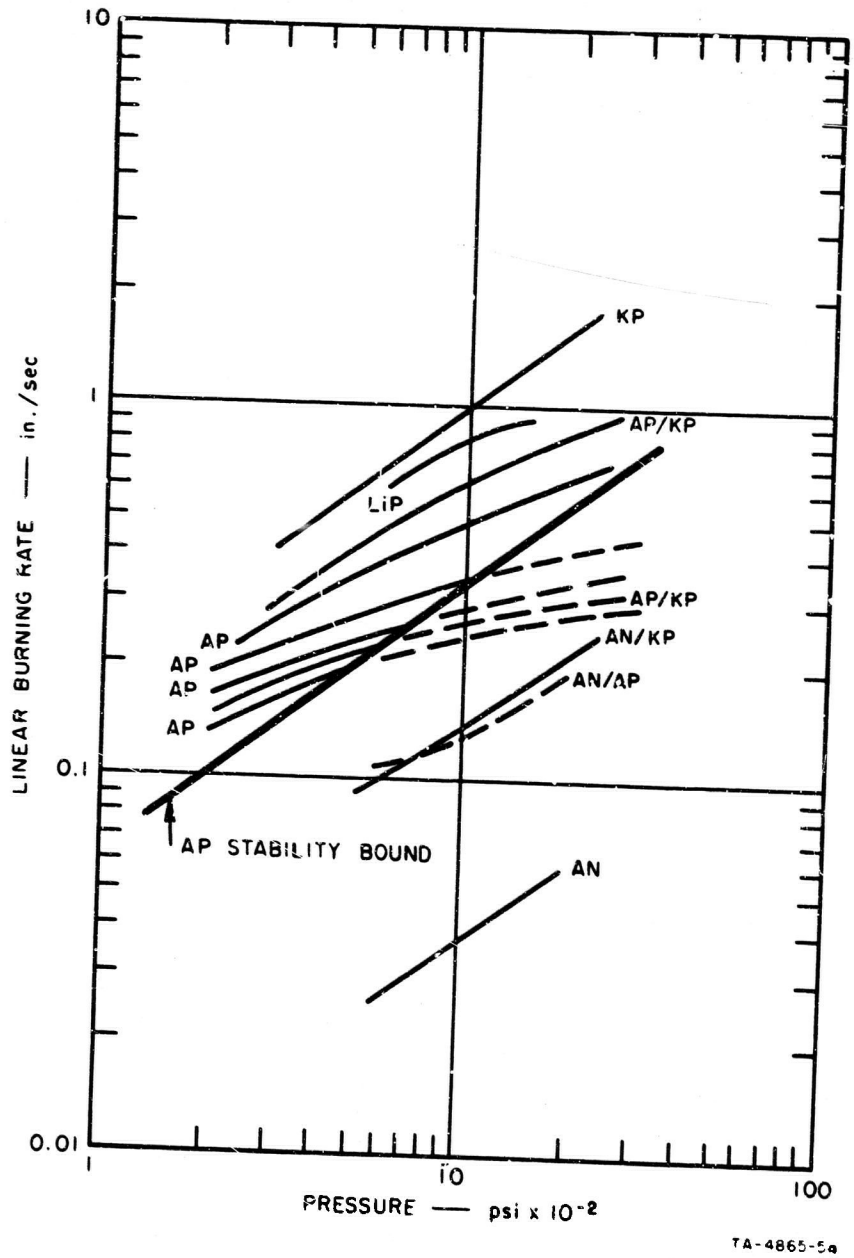

FIG. 21 INFLUENCE OF BURNING RATE AND COMPOSITION ON FINITE AMPLITUDE TRAVELING WAVE INSTABILITY; SOLID LINE STABLE REGIME, DOTTED LINE UNSTABLE REGIME FOR 5-INCH X 40-INCH MOTOR

IV CONCLUDING REMARKS

A. Theoretical Studies

The theoretical analysis developed during this program appears to be fully consistent with experimental observations pertaining to traveling wave, axial-mode combustion instability. In particular, it has been possible to explain the absence of instability in a 15 in. motor, the double-mode instability that invariably arises in our 82 in. motor, and the behavior of intermediate sizes, in terms of the theoretical frequency response of the propellant combustion mechanism. This achievement is of considerable importance, because it is the result of a quantitative comparison between theory and experiment. In addition, the theory provides a qualitative explanation for the experimentally determined boundary which separates the stable and unstable burning regions on a burning-rate vs. pressure diagram. It also offers a plausible explanation for the reversal of the stable and unstable regimes of composite and double-base propellants on such a diagram. These well-documented combustion instability characteristics appear to be a direct consequence of surface-coupled exothermic reactions, with composite and double-base propellants distinguished by differences in the chemical kinetics associated with such reactions.

One may legitimately question the applicability of a linearized theory to finite-amplitude traveling-wave phenomena. To answer this question it is necessary to consider, first, the actual objectives of a linearized theory, and second, the relative importance of errors that are inherent in the linear treatment, as compared to either errors in the determination of the associated thermochemical parameters, or experimental errors. First, the true role of linearized theory is to establish whether the underlying concepts (in this case, the combustion model) are consistent with observations. The criterion is good qualitative agreement, but not necessarily precise quantitative agreement. Second, we note that the theory has been used in this program to determine

the conditions under which the combustion process can support a traveling wave in a given configuration. The data show that such a wave introduces a traveling pressure pulse whose amplitude is about 20 percent of the undisturbed chamber pressure. This means that the terms neglected in the linear theory, which are on the order of $(\Delta p/p)^2$, represent less than a 5 percent error. This degree of accuracy cannot be achieved experimentally nor can it be achieved in evaluating parameters such as the activation energies, enthalpies of reaction, etc. Thus, the linear theory is appropriate on this basis.

To make the evaluation of theoretical applicability complete, however, it should be noted that the finite-amplitude traveling waves have a steep front. Therefore, they do not introduce a truly sinusoidal pressure pulse at the propellant surface, as has been assumed in the theory. The actual pressure pulse contains components of the higher harmonics. However, the evidence developed in this program indicates that the fundamental response is of predominant importance, for the traveling waves always are established at the fundamental resonance frequency of the propellant. Nevertheless, the harmonics, or the highly nonlinear aspects of the initial pulse, may be extremely important under some circumstances in initiating the instability. Thus, with the basic applicability of the combustion model strongly supported by the linearized theory, a nonlinear treatment would be of value in future studies.

Some investigators have suggested that velocity coupling may be very important in axial instability.[1,2] In the present analysis, as in all previous analyses known to us, only the pressure-coupling mechanism has been included in the combustion model. The results of this program indicate that pressure-coupling is the most important driving mechanism in traveling-wave instability, inasmuch as a relatively satisfactory description has been achieved by considering this mechanism alone. However, one can conceive of realistic situations in which velocity coupling could be important. In future studies we plan to attempt an appraisal of the role of velocity coupling through an appropriate modification of the combustion model and the linearized analysis of the response function.

Finally, it should be mentioned that the theoretical model described in the Appendix has also been used in our studies of combustion extinction, as explained in earlier technical reports on this investigation. In this way a relationship between combustion instability phenomena and extinction behavior has been established. That result justifies further efforts to relate the present studies to other problems, in both transient and steady combustion. This approach may ultimately make it possible to predict extinction behavior from instability observations, or instability limits from steady-state combustion measurements, for example. That such an accomplishment is a realistic possibility has been demonstrated during this program.

B. Experimental Studies and Stability Prediction

The experimental studies on finite amplitude wave axial mode instability have demonstrated, in association with the theoretical explanations developed, that the way has opened up to relating instability trends to propellant physical chemistry and to the ballistic design of the rocket motor. The importance of these facts to the rocket scientist cannot be underestimated, since it suggests that very early in any program useful data can be obtained from extremely small samples of propellants.

The experimental studies have involved the determination of solid phase heat release (using DTA or Differential Scanning Calorimeter techniques), the measurement of the propellant burning rate, measurement of thermal diffusivity, and the determination of solid phase kinetic data (adiabatic self-heating experiments).

Instability of composite propellants in the finite amplitude wave axial mode has been clearly indicated to be a shock wave whose propagation is supported by energy and mass addition at the walls in the wake of the wave. (The wave is driven at the recurrence rate, which can be supported by the frequency response band predicted from the chemical parameters of the combustion wave.) It has been reported previously

that changes in burning rate and operating pressure can be used to successfully design out combustion instability of the type studied.[1] In this present program it has been demonstrated that changes in the damping (wave reflection) characteristics of the head end can significantly improve rocket motor stability.

APPENDIX

FORMULATION OF THE COMBUSTION MODEL

The chief assumptions to be utilized in the following development are: (a) that the gas-phase reactions can be represented in terms of a single reaction of arbitrary order that obeys Arrhenius kinetics and responds instantaneously to pressure and temperature disturbances (i.e., time-dependent terms are omitted in the gas-phase equations); (b) that the Lewis number is unity in the gas phase; (c) that surface pyrolysis and surface-coupled exothermic or endothermic reactions follow Arrhenius laws; and (d) that the solid phase is essentially homogeneous with temperature-independent transport properties. For typical propellants assumption (a) is valid for chamber oscillations at frequencies of a few thousand cps or less. Most of the acoustic instability problems of greatest interest fall within this regime.

As (b) implies, the pyrolysis and surface-coupled reactions are assumed to occur in a surface layer of negligible thickness relative to the penetration depth of the temperature profile. It is difficult to evaluate the quantitative effect of assumptions (b), (c), and (d). However, it is important to remember that all analyses of this kind unavoidably rely on a highly simplified picture of the complex combustion process. Within this context these assumptions are fully justified, even necessary, because they permit a simplified mathematical formulation that is consistent with the underlying concepts.

The formulation begins with the equation governing heat conduction in the solid phase beyond the surface reaction zone:

$$\frac{\partial T}{\partial t} = r(t) \frac{\partial T}{\partial t} + K \frac{\partial^2 T}{\partial x^2} \qquad (1)$$

The propellant pyrolysis at the wall is assumed to follow an Arrhenius law so that the burning rate is related to wall temperature as follows:

$$r = ae^{-(E/RT_w)} \tag{2}$$

The following boundary condition is imposed upon the temperature:

$$x \to \infty; \quad T \to T_o \tag{3}$$

The remaining boundary condition is obtained through an energy-flux balance at the solid-gas interface. The net heat conducted into the unreacted solid propellant from the interface at the plane x = 0 is:

$$-k\left(\frac{\partial T}{\partial x}\right)_w = -k\left(\frac{\partial T}{\partial x}\right)_{g_w} - \rho_s r h_{g_w} + \rho_s r h_{s_w} + Q_H + Q_D \tag{4}$$

The first term on the right-hand side of the equality sign represents the energy coming from the gas phase; the second, the energy carried into the gas with the vaporizing propellant; the third, the energy carried by convection from the unreacted solid phase into the interface; the fourth, the energy released (positive) in heterogeneous decomposition reactions at the surface whose reaction rates depend upon the local gas-phase density; and the last, the energy released in solid-phase surface reactions with rates that are independent of gas-phase conditions. It is convenient to rewrite this expression as follows:[3]

$$-k\left(\frac{\partial T}{\partial x}\right)_w = -k\left(\frac{\partial T}{\partial x}\right)_{g_w} + \rho_s r[(c_s - c_p)T_w - L] + Q_H + Q_D \tag{5}$$

Denison and Baum[7] have obtained a solution to the gas-phase conservation equations by assuming that the complex gaseous reaction process can be represented by a single-step reaction of order n, where in some cases n may not be an integer. For now we shall retain their gas-phase solution, which yields the following expression for the heat flux from the gas phase to the wall:

$$-k\left(\frac{\partial T}{\partial x}\right)_{g_w} = \rho_s r[\epsilon_{r_w} Q_r - c_p(T_f - T_w)] \tag{6}$$

This solution also relates the instantaneous flow of reactant into the

gaseous reaction zone, $\rho_s r$, to the instantaneous gas-phase reaction rate, so that:

$$r = Cp^{\frac{n}{2}} T_f^{\frac{n}{2}+1} e^{-(E_f/2RT_f)} \tag{7}$$

The above derivation assumes that the surface-coupled reactions occur in a thin zone so that the surface heat release acts as a boundary condition on the solid phase. To derive a suitable kinetics description, the solid propellant can be thought of as containing possible reaction sites such that

$\rho_s r\chi$ = number of sites which undergo reaction per unit area of reaction zone per unit time

where χ is the number of sites which undergo reaction per unit mass of material. The heterogeneous heat release can now be expressed in terms of the above expression and an Arrhenius law as

$$Q_H = \rho_s r \, H_H \left(\frac{p}{T_w}\right)^m e^{-E_H/RT_w} \tag{8}$$

for a pressure-sensitive reaction. χ has been absorbed in H_H, the heat release per unit mass. In this respect H_H probably depends on the thickness of the surface reaction zone (which is related to $\rho_s r$), and on the specific nature of the pyrolysis process (which is also related to $\rho_s r$ ultimately). Thus, one might choose to write the above kinetics expression with $(\rho_s r)^y$ instead of $\rho_s r$. Then the exponent y becomes an unknown, and somewhat indirect, measure of the extent of surface reactions relative to gas-phase reactions. However, such a modification does not significantly alter the conclusions, and it has essentially no effect on the perturbation analysis given below. Therefore, until there emerges a more detailed understanding of the mechanism, any further complications of this type probably are unwarranted and will not be considered here.

Except that they are independent of the pressure, the other surface reactions follow a similar law:

$$Q_D = \rho_s r H_D e^{-E_D/RT_w} \tag{9}$$

Equations 5, 6, 8, and 9 can be combined to obtain:

$$-k\left(\frac{\partial T}{\partial x}\right)_w = \rho_s r \left[\epsilon_{r_w} Q_r - L - c_p T_f + c_s T_w + H_H \left(\frac{p}{T_w}\right)^m e^{-(E_H/RT_w)} + H_D e^{-(E_D/RT_w)}\right] \tag{10}$$

Equations 1, 2, and 7, with the boundary conditions of Eqs. 3 and 10, complete the mathematical representation of the combustion model in terms of the dependent variables T_f, T_w, and r. Owing to the nonlinear character of these equations, a closed-form solution cannot be obtained, in general. Consequently, we resort to a small-perturbation analysis, assuming that each dependent variable, as well as the pressure, is the sum of a steady and a perturbed component:

$$\begin{aligned} \tilde{p} &= \bar{p}\ (1 + \tilde{p}) \\ T_f &= \bar{T}_f\ (1 + \tilde{T}_f) \\ T_w &= \bar{T}_w\ (1 + \tilde{T}_w) \\ r &= \bar{r}\ (1 + \tilde{r}) \end{aligned} \tag{11}$$

where, for example, $\tilde{p}$ is the ratio $[p(t) - \bar{p}]/\bar{p} \ll 1$. By introducing these expressions into Eqs. 1, 2, 3, 7, and 10, and retaining only first-order terms in the perturbed quantities, one can obtain a set of linear equations. The solution to these equations gives the first-order response of the combustion mechanism to a perturbation in the chamber pressure.

By modifying the parameters α and B defined by Denison and Baum,[3] it is possible to generalize the analysis by these investigators; their

mathematical solution describes the behavior of the combustion model formulated above when it is expressed in terms of the following transformation:

$$\left.\begin{aligned} \alpha &= \alpha_o - \frac{\theta_s}{A} \\ B &= \frac{\alpha_o B_o + m\theta_H}{\alpha_o - \theta_s/A} \end{aligned}\right\} \tag{12}$$

where:

$$A = A_o = \frac{E_w}{R\bar{T}_w}\left(\frac{\bar{T}_w - T_o}{\bar{T}_w}\right) \tag{13}$$

$$\alpha_o = \frac{c_p \bar{T}_f}{c_s (\bar{T}_w - T_o)} \frac{1}{\left(\frac{n+2}{2} + \frac{E_f}{2R\bar{T}_f}\right)}$$

$$\theta_s = \left(\frac{E_H}{R\bar{T}_w} - m\right)\theta_H + \frac{E_D}{R\bar{T}_w}\,\theta_D \tag{13}$$

$$\theta_H = \frac{H_H}{c_s \bar{T}_w}\left(\frac{P}{\bar{T}_w}\right)^m \exp\left(-E_H/R\bar{T}_w\right) = \frac{Q_H}{Q_T}\left(\frac{\bar{T}_w - T_o}{\bar{T}_w}\right) \tag{14}$$

$$\theta_D = \frac{H_D}{c_s \bar{T}_w} \exp\left(-E_D/R\bar{T}_w\right) = \frac{Q_D}{Q_T}\left(\frac{\bar{T}_w - T_c}{\bar{T}_w}\right) \tag{15}$$

The subscript zero on α, B, and A denotes the value, as defined by Denison and Baum,[3] for zero surface-coupled heat release. It is also convenient to define an overall, steady-state pressure exponent for the propellant, ν, in terms of the usual empirical burning rate formula, $\bar{r} = cp^{\nu}$. It follows that:

$$\nu = \frac{\alpha_o \frac{n}{2} + m\theta_H T_w/(T_w - T_o)}{\alpha_o - \theta_s/A} \qquad (16)$$

Note that when there are no surface-coupled reactions, $\theta_s = \theta_H = 0$ and the analysis reduces to that of Denison and Baum,[3] in which case the pressure exponent $\nu = n/2$ (n is the order of the gas-phase reaction).

It can be shown that the parameter θ_s is roughly proportional to the fraction of the total heat release that occurs in surface-coupled reactions and greater by approximately an order of magnitude. Thus, if ten percent of the total heat release in the combustion process occurs in surface-coupled reactions, $\theta_s \approx 1$. The relationship between θ_H and the fraction released in surface reactions with pressure-dependent kinetics (e.g. heterogeneous reactions) is indicated by Eq. 14; that between θ_D and the pressure-independent surface reactions (e.g. decomposition) appears in Eq. 15.

The transient behavior of the present combustion model is easily obtained from Denison and Baum's solution by using the transformation given in Eq. 12. Only a brief summary will be presented here.

A given propellant may be characterized in terms of three parameters; A, which relates to the surface decomposition kinetics; α, which relates to the gas-phase kinetics; and θ_s, which relates to the distribution of heat release between surface-coupled and gas-phase reactions. Relative to the behavior with no surface-coupled reactions ($\theta_s = 0$), a negative θ_s extends the range of A and of α for which the propellant is inherently stable in the "self-excited" mode;[3] a positive θ_s reduces this range. As Eq. 13 shows, the sign of θ_s is determined by the relative magnitudes of $E_H/R\bar{T}_w$, m, and $E_D/R\bar{T}_w$, as well as by the signs of θ_H and θ_D (which are positive for exothermic reactions, negative for endothermic reactions).

Of course all practical propellants must have a stable self-excited mode, although some may be closer to the unstable limit than others, depending on their specific values of A, α, and θ_s. The stable zone is

described by the relation·

$$q^2 - q - 2A < 0 \qquad (17)$$

where

$$q = 1 + \theta_s + A(1 - \alpha_o)$$

Thus, only values of A, α, and θ_s that satisfy Eq. 17 are of practical importance.

The "steady oscillatory" mode corresponds to the response of a propellant, whose parameters satisfy the inequality of Eq. 17, to pressure perturbations. This response may be represented in terms of the normalized (by the pressure index ν) acoustic response function, $\tilde{m}/\nu\tilde{p}$. The real part of the complex response function is of greater practical significance, because it is the component of the mass perturbation which is in phase with the pressure perturbation that tends to drive the oscillations. The analysis shows that the resonance amplitudes of the real part and of the complex response function are almost equal when the latter is less than about 10. Relative to the case where surface reactions are absent ($\theta_s = 0$), an increase in θ_s (positive θ_s) increases the amplitude of the response function; a decrease (negative θ_s) reduces the amplitude, i.e., tends to stabilize the propellant.

To relate this conclusion to actual propellant combustion phenomena, it will be helpful to consider a physical interpretation of the surface reaction kinetics. For composite propellants we may envision the surface reaction zone as encompassing, first, pyrolysis of the propellant (described by Eq. 2) and subsequently, surface-coupled reactions among the pyrolysis products (described in Eqs. 8 and 9). Thus, the activation energies E_H and E_D associated with Eqs. 8 and 9 represent an overall description of a complicated sequence of events, which may include mixing between the various macroscopic constituents of the composite propellant, as well as reaction steps. In contrast, with a double-base propellant there is no reason to distinguish surface-coupled energetic

reactions from pyrolysis reactions, because the constituents are intermixed on a molecular scale. Thus, the pyrolysis and other reactions may be considered as a single sequence, with a single activation energy, E, Characterizing the rate-controlling step, and with $E_H = E_D = 0$. A possible exception might occur with heterogeneous reactions, which could call for a very small value of E_H associated with molecular mixing between gas-phase constituents and pyrolysis products.

In summary, a composite propellant generally corresponds to $E_H > 0$ and/or $E_D > 0$, whereas for a double-base propellant $E_H = E_D = 0$ (with the relatively minor exception noted above). When there are exothermic surface-coupled reactions ($\theta_H > 0$, $\theta_D > 0$), for example, it follows from Eq. 13 that $\theta_s > 0$ for composite propellants, whereas $\theta_s < 0$ (unless $E_H/RT_w > m$ owing to molecular mixing) for double-base propellants. It follows that exothermic surface-coupled reactions tend to destabilize composite propellants (by increasing the response amplitude), while they tend to stabilize double-base propellants. This rather remarkable theoretical conclusion is entirely consistent with our experimental observation that the stable burning regimes of composite and double-base propellants are reversed. The effect of surface-coupled reactions may well explain this surprising observation.

REFERENCES

1. E. L. Capener, L. A. Dickinson, R. J. Kier, "Driving Processes of Finite Amplitude Axial Mode Instability in Solid Propellant Rockets," in course of publication AIAA J., May 1967.

2. E. L. Capener, L. A. Dickinson, R. J. Kier, G. A. Marxman, "Response of a Burning Propellant Surface to Erosive Transients," AFOSR Contract No. AF 49(638)-1507, March 15, 1966.

3. M. R. Denison and E. Baum, "A Simplified Model of Unstable Burning in Solid Propellants," ARS J. 31, 1112 (1961).

4. A. J. Sabadell, J. Wenograd, M. Summerfield, "Measurement of Temperature Profile Through Solid Propellant Flames Using Fine Thermocouples," AIAA J. 3, No. 9 (September 1965).

5. Stanley F. Saurer, "Propellant Chemistry," Reinhold Publishing Co., N. Y., p. 296, 1966.

6. Ronald Reed, L. Weber, and B. Gottfried, "Differential Thermal Analysis and Reaction Kinetics," Industrial and Engineering Chemistry Fundamentals 4, No. 1, p. 38 (February 1965).

7. R. B. Beyer and N. Fishman, "Solid Propellant Ignition Studies with High Flux Radiant Energy as a Thermal Source, "Progress in Astronautics and Rocketry 1, Solid Propellant Rocket Research, pp. 673-692, Academic Press, 1960.

8. N. Fishman, "Solid Propellant Ignition Studies," Stanford Research Institute Final Report under Contract No. AF 04(611)-10534, Report No. AFRPL-TR-65-213, November 5, 1965.

9. L. A. Povinelli, "Study of Composite Solid-Propellant Flame Structure Using A Spectral Radiation Shadowgraph Technique," AIAA J. 3, 1593-1598 (1965).

10. R. H. Woodward Waische, "Spectrographic Studies of Solid-Propellant Flames (U)," Rohm and Haas Co., Special Report No. S-111, October 1966, Contract No. DA-01-021 AMC 11536(2). (Confidential)

11. R. W. Hart and F. T. McClure, "Theory of Acoustic Instability in Solid-Propellant Rocket Combustion," Tenth Symposium (International) on Combustion, pp. 1047-1065, The Combustion Institute, Pittsburgh, 1965.

12. E. W. Price, "Experimental Solid Rocket Combustion Instability," Tenth Symposium (International) on Combustion, pp. 1067-1082, The Combustion Institute, Pittsburgh, 1965.

13. R. W. Hart and F. T. McClure, "Combustion Instability: Acoustic Interaction with a Burning Propellant Surface," J. Chem. Phys. 30, 1501-1514 (1959).

14. F. A. Williams, "Response of a Burning Solid to Small-Amplitude Pressure Oscillations," J. Appl. Phys. 33, 3153-3166 (1962).

15. J. C. Friedly and E. E. Petersen, "Influence of Combustion Parameters on Instability in Solid Propellant Motors: Part I. Development of Model Linear Analysis," AIAA J. 4, 1604-1610 (1966); "Part II. Nonlinear Analysis," AIAA J. 4, 1932-1937 (1966).

16. F. E. C. Culick, "Calculation of the Admittance Function for a Burning Surface," presented at 3rd ICRPG Combustion Conference, J. F. Kennedy Space Center, Cocoa Beach, Florida, October 1966.

17. S. S. Novikov and Yu. S. Ryazantsev, "The theory of steady-state velocity of propagation of an exothermal reaction front in a condensed medium," Zh. Prikladnoy Mekhaniki Fiziki, No. 3, 43-48 (1965).

18. E. L. Caponer, et al, "Response of a Burning Propellant Surface to Erosive Transients," Third Quarterly Report, AFOSR Contract AF 49(638)-1665, October 1966.

UNCLASSIFIED

Security Classification

DOCUMENT CONTROL DATA - R & D

(Security classification of title, body of abstract and indexing annotation must be entered when the overall report is classified)

1. ORIGINATING ACTIVITY (Corporate author)
Stanford Research Institute
333 Ravenswood Avenue
Menlo Park, California 94025

2a. REPORT SECURITY CLASSIFICATION
Unclassified

2b. GROUP

3. REPORT TITLE

RESPONSE OF A BURNING PROPELLANT SURFACE TO EROSIVE TRANSIENTS

4. DESCRIPTIVE NOTES (Type of report and inclusive dates)
Annual Report, January 1, 1966 - December 31, 1966

5. AUTHOR(S) (First name, middle initial, last name)
Erwin L. Capener
Lionel A. Dickinson
Roger J. Kier
Gerald A. Marxman
Charles E. Wooldridge

6. REPORT DATE	7a. TOTAL NO. OF PAGES	7b. NO. OF REFS
	80	18

8a. CONTRACT OR GRANT NO.	9a. ORIGINATOR'S REPORT NUMBER(S)
AF 49(638)-1665	FRU-5818
b. PROJECT NO. SRI No. FRU-5818	
c.	9b. OTHER REPORT NO(S) (Any other numbers that may be assigned this report)
d.	

10. DISTRIBUTION STATEMENT
Subject to special export control and each transmittal to foreign governments or foreign nationals may be made only with prior approval of AFOSR.

11. SUPPLEMENTARY NOTES	12. SPONSORING MILITARY ACTIVITY
	Air Force Office of Scientific Research Washington, D. C. 20333

13. ABSTRACT

The study of the combustion instability of solid propellants has as its ultimate goal the development of a method for predicting whether a new propellant will be susceptible to combustion instability. In the studies done under this present contract, significant progress has been made in correlating finite-amplitude axial-mode instability with a theoretical analysis of the combustion wave. When laboratory derived physical-chemical propellant data are substituted in the appropriate expressions, it has proved possible to predict in a qualitative manner the unstable response of a propellant.

The studies this year have been concerned with improving the combustion model, interpreting the fluid dynamic phenomena, and experimentally determining the magnitude of critical ballistic parameters. In order to verify that solid-phase reactions were occurring, differential thermal analysis studies were performed on selected propellants at pressures up to 70 atmospheres. A quadrapole mass spectrometer was used to distinguish between condensed-phase and gas-phase reactions. With ammonium perchlorate propellants, a solid-phase heat release of up to 200 calories per gram was observed.

An examination of the wave structure obtained in both tubular and opposed slab rocket motors indicates that the finite amplitude wave is a shock wave (supported by mass and energy addition in the wake).

In the continuing development of the analytical model of the combustion wave, the justification of the physical assumptions made in developing a mathematically tractable theory have been critically reviewed and compared with those of other workers

DD FORM 1 NOV 65 1473

UNCLASSIFIED

Security Classification

14. KEY WORDS	LINK A		LINK B		LINK C	
	ROLE	WT	ROLE	WT	ROLE	WT
Combustion Instability						
Combustion Model						
Composite Propellants						
Double Base Propellants						
Propellant Response						
Solid Phase Reactions						
Solid Propellants						